




# $\alpha$ -Synuclein in blood exosomes immunoprecipitated using neuronal and oligodendroglial markers distinguishes Parkinson's disease from multiple system atrophy

Suman Dutta<sup>1</sup> · Simon Hornung<sup>1,14</sup> · Adira Kruayatidee<sup>1</sup> · Katherine N. Maina<sup>1</sup> · Irish del Rosario<sup>2</sup> · Kimberly C. Paul<sup>2</sup> · Darice Y. Wong<sup>1</sup> · Aline Duarte Folle<sup>2</sup> · Daniela Markovic<sup>3</sup> · Jose-Alberto Palma<sup>4</sup> · Geidy E. Serrano<sup>5</sup> · Charles H. Adler<sup>6</sup> · Susan L. Perlman<sup>1</sup> · Wayne W. Poon<sup>7</sup> · Un Jung Kang<sup>4</sup> · Roy N. Alcalay<sup>8</sup> · Miriam Sklerov<sup>9</sup> · Karen H. Gyls<sup>10,12</sup> · Horacio Kaufmann<sup>4</sup> · Brent L. Fogel<sup>1,11,12</sup> · Jeff M. Bronstein<sup>1,12</sup> · Beate Ritz<sup>2,12</sup> · Gal Bitan<sup>1,12,13</sup> 

Received: 31 October 2020 / Revised: 1 May 2021 / Accepted: 3 May 2021  
© The Author(s) 2021

## Abstract

The diagnosis of Parkinson's disease (PD) and atypical parkinsonian syndromes is difficult due to the lack of reliable, easily accessible biomarkers. Multiple system atrophy (MSA) is a synucleinopathy whose symptoms often overlap with PD. Exosomes isolated from blood by immunoprecipitation using CNS markers provide a window into the brain's biochemistry and may assist in distinguishing between PD and MSA. Thus, we asked whether  $\alpha$ -synuclein ( $\alpha$ -syn) in such exosomes could distinguish among healthy individuals, patients with PD, and patients with MSA. We isolated exosomes from the serum or plasma of these three groups by immunoprecipitation using neuronal and oligodendroglial markers in two independent cohorts and measured  $\alpha$ -syn in these exosomes using an electrochemiluminescence ELISA. In both cohorts,  $\alpha$ -syn concentrations were significantly lower in the control group and significantly higher in the MSA group compared to the PD group. The ratio between  $\alpha$ -syn concentrations in putative oligodendroglial exosomes compared to putative neuronal exosomes was a particularly sensitive biomarker for distinguishing between PD and MSA. Combining this ratio with the  $\alpha$ -syn concentration itself and the total exosome concentration, a multinomial logistic model trained on the discovery cohort separated PD from MSA with an AUC = 0.902, corresponding to 89.8% sensitivity and 86.0% specificity when applied to the independent validation cohort. The data demonstrate that a minimally invasive blood test measuring  $\alpha$ -syn in blood exosomes immunoprecipitated using CNS markers can distinguish between patients with PD and patients with MSA with high sensitivity and specificity. Future optimization and validation of the data by other groups would allow this strategy to become a viable diagnostic test for synucleinopathies.

**Keywords** Biomarker · Extracellular vesicles · Synucleinopathy · Biofluid

## Introduction

Synucleinopathies are neurodegenerative diseases characterized by abnormal accumulation of intracellular  $\alpha$ -syn aggregates. In Parkinson's disease (PD) and dementia with Lewy bodies (DLB),  $\alpha$ -syn accumulates in intraneuronal Lewy bodies and Lewy neurites, whereas in multiple system atrophy (MSA),  $\alpha$ -syn deposits primarily as glial cytoplasmic inclusions (GCIs) in oligodendrocytes [8, 45, 67].

Accumulation and deposition of  $\alpha$ -syn also occur in other neurodegenerative diseases and conditions, such as Alzheimer's disease (AD), pure autonomic failure, rapid eye movement sleep behavioral disorders, traumatic brain injury, and neuroaxonal dystrophies [29, 41, 44]. Though synucleinopathies have distinct symptoms and underlying pathophysiology, during early stages, they often are misdiagnosed due to overlapping symptoms with other synucleinopathies, atypical parkinsonian tauopathies, spinocerebellar ataxias, and/or dementias [18, 46, 48].

The diagnosis accuracy of PD is approximately 80% and is lower in new cases [1, 4]. The rates of misdiagnosis are higher for the rarer synucleinopathies [57, 62]. A retrospective post-mortem study found that about one in four patients

✉ Gal Bitan  
gbitan@mednet.ucla.edu

Extended author information available on the last page of the article

who received the clinical diagnosis of PD by a general neurologist actually was a misdiagnosis of MSA or progressive supranuclear palsy (PSP) [33]. A separate autopsy study of 134 patients diagnosed with MSA found 71% accuracy in patients diagnosed with probable MSA and 60% in those diagnosed with possible MSA [34].

The clinical diagnosis of MSA currently is based on sets of autonomic and motor symptoms that provide variable degrees of diagnostic certainty [23, 68]. Compared to PD, patients with MSA have more severe, generalized, and rapidly progressive autonomic failure, particularly in the early stages of disease. Thus, autonomic testing can be helpful to assist in the diagnosis of MSA [50, 51]. For example, abnormal thermoregulatory sweat testing has a high specificity for distinguishing MSA from PD or DLB. Preserved myocardial  $^{123}\text{I}$ -Iobenguane imaging is a useful supporting feature of MSA, as it is typically impaired in PD and DLB, and an elevated post-void bladder residual volume, particularly in early stages, is highly indicative of MSA [51]. However, autonomic dysfunction also can be a confounder [49]. For example, the presence of neurogenic orthostatic hypotension is not useful for discriminating MSA from PD as it can be present in all synucleinopathies [38, 50].

Multiple attempts to develop imaging and cerebrospinal fluid (CSF)-based biomarkers for synucleinopathies [10, 56, 59] have been made to date, but due to their lack of specificity and/or invasive nature, none has translated yet into regular clinical practice. Currently, a definite diagnosis can only be made at autopsy [23, 55]. Development of sensitive and specific biomarkers for synucleinopathies therefore is an urgent public health need for proper disease diagnosis, establishment of appropriate inclusion and exclusion criteria for clinical trials, and use of pharmacodynamic measures of treatment effects.

Extracellular vesicles (EVs), including exosomes and ectosomes, are heterogeneous vesicles released by virtually all cell types. They contain parent-cell-specific cargoes of proteins, lipids, and nucleic acids [63]. Exosomes are the smallest and most abundant EVs. They provide an important mode of intercellular communication and a rich source of biomarkers [31, 39, 53]. Recent studies have shown that exosomes were involved in interneuronal and neuron–glia communication [6, 20, 21].  $\alpha$ -Syn has been shown to transfer via exosomes among different brain cells [3, 12], seed aggregation [27], and induce apoptosis in recipient cells [13, 15].

Recently, several studies have demonstrated that exosomes isolated from serum or plasma by immunoprecipitation using neuronal markers carried cargo from their putative cells of origin through the blood–brain barrier and thus could provide a “window” into pathologic processes in the brain, offering a major advancement in analyzing brain biomarkers non-invasively [17, 24, 25, 60, 61]. Although over 50 papers using this strategy have been published since

2014, to date, no study has demonstrated unequivocally that the origin of the exosomes indeed was CNS neurons. Therefore, we refer to these exosomes as putatively originating in the CNS.

Shi et al. [61] have reported a significantly higher concentration (~twofold) of  $\alpha$ -syn in putative neuronal exosomes isolated from the plasma of patients with PD compared to healthy individuals, yet a substantial overlap was found between the groups. More recently, Jiang et al. [32] used a combination of  $\alpha$ -syn and clusterin concentrations measured in putative neuronal exosomes and found that they separated efficiently patients with PD from those with atypical parkinsonian syndromes. The study included 14 patients with MSA in which the putative neuronal exosomal  $\alpha$ -syn concentrations were significantly lower than in patients with PD. Yu et al. measured  $\alpha$ -syn concentrations in putative neuronal and oligodendroglial exosomes, the latter isolated by immunoprecipitation from patient plasma using the oligodendrocyte marker 2,3-cyclic nucleotide-3-phosphodiesterase (CNPase), as a potential diagnostic biomarker for separating patients diagnosed with PD ( $N=34$ ) from those diagnosed with MSA ( $N=32$ ) [70].  $\alpha$ -Syn concentrations again were found to be lower in the exosomes from patients with MSA than in those with PD, yet the differences were small and the degree of overlap between the groups was high.

Because  $\alpha$ -syn accumulates primarily in neurons in PD and oligodendrocytes in MSA, we hypothesized that comparing its levels in putative neuronal and oligodendroglial exosomes might allow differentiating MSA from PD. We used a different marker from the one chosen by Yu et al., myelin oligodendrocyte glycoprotein (MOG), for isolation of oligodendroglial exosomes. Using this marker, we found in both diseases a significant elevation of  $\alpha$ -syn concentration in putative oligodendroglial exosomes compared to healthy controls.  $\alpha$ -Syn concentrations were particularly high in the MSA group compared to the control and PD groups. The ratio between  $\alpha$ -syn concentrations in putative oligodendroglial versus neuronal exosomes was found to be a sensitive biomarker for distinguishing between PD and MSA.

## Materials and methods

### Study populations

#### Discovery cohort

Serum samples were collected initially for a discovery cohort from 51 healthy controls, 50 patients with PD, and 30 patients with MSA. The sample sources for this cohort included: (1) the Parkinson's Environment and Genes (PEG) study, UCLA; (2) the Institute for Memory Impairments and Neurological Disorders, UC Irvine; (3) the Clinical

Neurogenomics Research Center, UCLA; and (4) the Dysautonomia Center, New York University School of Medicine. Except for one sample from NYU, the control samples were collected as part of the PEG study at the same time of collecting patient samples and were primarily from patient spouses or other relatives. After discovering that samples stored for > 5 years had reduced signal (Supplementary Information), all of these samples were replaced with new samples stored < 5 years. The final composition of the discovery cohort is summarized in Table 1. Blood-collection procedures were approved by the respective Human Subjects Committees at each institution and informed consent was obtained from all participants.

### Postmortem cohort

Serum samples collected post-mortem with post-mortem interval (PMI) 1.5–6 h from 49 patients with PD and 12 patients with MSA were obtained from Banner Sun Health Research Institute. The diagnosis in this cohort was validated pathologically in each case as described previously [5].

### Validation cohort

Serum or plasma samples were collected from 50 healthy controls, 50 patients with PD, and 50 patients with MSA. Each sample was from a unique donor. The samples sources for this cohort were similar to the discovery cohort, with an addition of two additional sources: The Department of Neurology, Columbia University and the Easton Center biobank

at UCLA. About half of the control samples were again from the PEG study, whereas the other half were from Columbia and were collected as part of a different project from the one supplying the MSA samples. After discovering that samples stored for > 5 years had reduced signal (Supplementary Information), all of these samples were replaced with new samples stored < 5 years. The final composition of the validation cohort is summarized in Table 2.

### PD diagnosis

Board-certified neurologists diagnosed PD according to the Movement Disorders Society clinical diagnostic criteria for PD [52]. At baseline and each follow-up, UCLA movement disorder specialists (providing 93% of the PD samples used in this study) confirmed a diagnosis of idiopathic PD and evaluated motor features using the Unified Parkinson's Disease Rating Scale (UPDRS parts I, III, and IV) and Höhn and Yahr (H&Y) staging. At each time point, > 80% of the participants were evaluated in an 'off' ( $\geq 12$  h) medication state. For those 'on', a correction factor was added to their UPDRS-III total score, equal to the mean difference of 'off' and 'on' scores in all patients. The average of the whole sample also was used to impute missing items (mainly due to disability impeding evaluation of specific items such as 'arise from chair'). The MDS version of the UPDRS-III was adopted in 2016, and thus, scores derived from this scale were corrected by subtracting seven points according to the method of Hentz et al. [30]. Samples provided by NYU were all from patients off medication and the patients were evaluated using the MDS version of the UPDRS-III. Cognitive

**Table 1** Demographic and clinical data for final discovery cohort

|  | All samples         | Control             | PD                 | MSA (C:P)                       |
|--|---------------------|---------------------|--------------------|---------------------------------|
| Total samples                                  | 131                 | 50                  | 51                 | 30 (26:4)                       |
| Age <sup>a</sup> (range)                       | 66.3 ± 11.1 (35–90) | 63.2 ± 12.2 (35–86) | 71.5 ± 9.5 (37–90) | 62.7 ± 8.3 (46–79)              |
| Sex (male:female)                              | 67:64               | 22:28               | 32:19              | 13:17                           |
| Disease duration in years <sup>a</sup> (range) | 7.0 ± 4.7 (0–19)    |                     | 8.4 ± 5.0 (0–19)   | 4.4 ± 2.6 (0–10)                |
| Race/ethnicity <sup>b</sup>                    | As <sup>c</sup> – 8 | As – 1              | As – 0             | As – 7                          |
|  | B – 2               | B – 0               | B – 1              | B – 1                           |
|  | H – 6               | H – 4               | H – 1              | H – 1                           |
|  | HN – 14             | HN – 6              | HN – 8             | HN – 0                          |
|  | NA – 3              | NA – 2              | NA – 1             | NA – 0                          |
|  | ND – 2              | ND – 1              | ND – 0             | ND – 1                          |
|  | W – 96              | W – 36              | W – 40             | W – 20                          |
|  |                     |                     | 25.4 ± 15.3 (0–59) |                                 |
| UPDRS <sup>d</sup> motor (range)               |                     |                     |                    |                                 |
| H&Y <sup>d</sup> (range)                       | 2.7 ± 1.1 (1–5)     |                     | 2.5 ± 1.0 (1–5)    | 3.8 ± 1.0 (2–5)                 |
| MMSE <sup>d</sup> (range)                      |                     |                     | 26.5 ± 6.2 (0–30)  | 26.5 ± 9.3 (10–30) <sup>e</sup> |

<sup>a</sup>Mean ± SD. <sup>b</sup>As—Asian; B—Black; H—Hispanic; HN—Hispanic, non-White; NA—Native American, ND—non-disclosed; W—White.

<sup>c</sup>Korea—2, Philippines—1, Taiwan—1, Vietnam—1, Undefined Asian—3. <sup>d</sup>UPDRS—Unified Parkinson's disease rating scale, H&Y—Höhn and Yahr rating scale, MMSE—Mini-Mental State Examination. <sup>e</sup>Converted from Montreal Cognitive Assessment (MoCA) according to Lawton et al. [36]

**Table 2** Demographic and clinical data for final validation cohort

|  | All Samples         | Control            | PD                  | MSA (C: P:mixed)                |
|--|---------------------|--------------------|---------------------|---------------------------------|
| Total samples                                  | 154                 | 51                 | 53                  | 50 (33:13:4)                    |
| Age <sup>a</sup> (range)                       | 67.3 ± 9.8 (40–88)  | 66.6 ± 8.9 (44–88) | 72.0 ± 10.2 (40–88) | 62.9 ± 7.9 (47–79)              |
| Sex (male:female)                              | 82:72               | 23:28              | 33:20               | 26:24                           |
| Disease duration in years <sup>a</sup> (range) | 6.9 ± 4.1 (1–26)    |                    | 8.1 ± 3.8 (2–20)    | 5.6 ± 4.0 (1–26)                |
| Race/ethnicity <sup>b</sup>                    | As <sup>c</sup> – 8 | As – 1             | As – 1              | As – 6                          |
|  | B – 4               | B – 0              | B – 0               | B – 4                           |
|  | H – 22              | H – 10             | H – 11              | H – 1                           |
|  | HN – 0              | HN – 0             | HN – 0              | HN – 0                          |
|  | NA – 5              | NA – 1             | NA – 4              | NA – 0                          |
|  | ND – 6              | ND – 4             | ND – 1              | ND – 1                          |
|  | W – 109             | W – 35             | W – 36              | W – 38                          |
| UPDRS <sup>d</sup> motor (range)               |                     |                    | 26.0 ± 13.3 (0–49)  |                                 |
| H&Y <sup>d</sup> (range)                       | 2.3 ± 0.9 (0–5)     |                    | 2.3 ± 0.8 (0–4)     | 3.0 ± 2.8 (1–5)                 |
| MMSE <sup>d</sup> (range)                      |                     |                    | 27.6 ± 2.3 (18–30)  | 28.0 ± 1.7 (24–30) <sup>e</sup> |

<sup>a</sup>Mean ± SD. <sup>b</sup>As—Asian; B—Black; H—Hispanic; HN—Hispanic, non-White; NA—Native American, ND—non-disclosed; W—White. <sup>c</sup>Undefined Asian—8. <sup>d</sup>UPDRS—Unified Parkinson's disease rating scale, H&Y—Höhn and Yahr rating scale, MMSE—Mini-Mental State Examination. <sup>e</sup>Converted from Montreal Cognitive Assessment (MoCA) according to Lawton et al. [36]

function was assessed using the Mini-Mental State Examination (MMSE).

### MSA diagnosis

Patients diagnosed with MSA fulfilled current consensus criteria for possible or probable MSA [23]. Detailed information was collected on demographics, risk factors, chronic diseases, and medication use. Patients were assessed using the Unified Multiple System Atrophy Rating Scale (UMSARS) or Scale for Assessment and Rating of Ataxia (SARA). Whenever possible, patients were examined off antiparkinsonian medications. Cognitive function was assessed using the MMSE or Montreal Cognitive Assessment (MoCA).

### Serum collection

Peripheral blood from living persons was drawn by venipuncture using a BD Vacutainer push-button blood-collection kit and left to coagulate in silicone-coated serum-collection tubes for 15–20 min. After centrifugation at 1500g for 15 min at 4 °C, the serum was collected and either processed immediately or aliquoted and stored at – 80 °C.

Postmortem serum was obtained as described previously [5]. Briefly, blood was drawn from the left ventricle by a transthoracic puncture using 30-mL, disposable, polyethylene syringes fitted with 8-cm long, 18-gauge needles. Serum was separated from the blood using standard serum separator vacuum tubes (7 mL) prior to 10 min centrifugation,

aliquoted into 0.5-mL polyethylene microcentrifuge tubes, and stored at – 80 °C.

### Plasma collection

Plasma samples were obtained as described previously [2]. Briefly, peripheral blood was drawn by venipuncture and collected into EDTA tubes. Within 30 min of collection, the plasma tubes underwent centrifugation at 4 °C for 15 min at 1500g. The plasma then was aliquoted into 0.5 mL aliquots (control samples) or 1.0 mL aliquots (MSA samples) and stored at – 80 °C.

### Measurement of serum hemoglobin

Hemoglobin concentration was measured using a hemoglobin assay kit (Sigma-Aldrich) according to the manufacturer's instructions. Fifty microliters of undiluted serum/plasma samples were used, and hemoglobin concentration was quantified with reference to a standard curve generated using freshly prepared stock hemoglobin.

### EV isolation

Frozen serum or plasma samples were thawed on ice. Protease and phosphatase inhibitor cocktails (PPI, Sigma-Aldrich) were added immediately, and the samples were centrifuged at 2000g for 10 min at 4 °C to precipitate any cells or cell-debris remnants. Clear supernates (250 µL) then were mixed gently with 63 µL of an ExoQuick Exosome Precipitation Solution (System Biosciences) and incubated on



ice for 1 h, followed by centrifugation at 1500g for 30 min at 4 °C. The resulting pellets were suspended in pre-chilled PBS containing 1% (w/v) bovine serum albumin (BSA) and PPI for subsequent enrichment steps.

### Exosome concentration measurement

Exosome concentration was measured indirectly using the ExoELISA Ultra CD81 assay (System Biosciences). After isolation, exosomes were resuspended in PBS supplemented with PPI. Five hundred µg of total protein of each sample and CD81 standards were loaded onto a 96-well plate and incubated for 1 h at 37 °C. The wells then were washed thrice for 5 min and incubated with an anti-CD81 primary antibody in blocking buffer with gentle agitation at room temperature (RT). Wells then again were washed thrice for 5 min and incubated with a horseradish peroxidase (HRP)-conjugated secondary antibody in blocking buffer with gentle agitation at RT for 1 h. Then, 50 µL of tetramethylbenzidine (TMB) substrate were added to each well and incubated for 10 min with shaking at RT. Stop buffer was added and absorbance was measured at 450 nm using a Synergy HTX plate reader (BioTek, USA).

### Immunoprecipitation (IP) of exosomes using neuronal and oligodendroglial markers

Two µg each of anti-L1 cell-adhesion molecule (L1CAM, clone 5G3, Santa Cruz Biotechnology) for enrichment of neuronal exosomes, anti-myelin oligodendrocyte glycoprotein (MOG, clone D-2, Santa Cruz Biotechnology) for enrichment of oligodendroglial exosomes, or normal mouse IgG (Life Technologies) as a negative control were used to coat 1 mg of M-270 epoxy Dynabeads using a Dynabeads Antibody Coupling Kit (Life Technologies) overnight at 37 °C with gentle rotation following the manufacturer's instructions. Antibody-coated beads then were mixed gently with the isolated serum/plasma EVs in chilled phosphate-buffered saline (PBS), pH 7.4, containing 1% (w/v) BSA and PPI and incubated overnight at 4 °C with gentle rotation. The bead-attached exosomes then were washed with 1 mL of 0.1% (w/v) BSA in PBS, pH 7.4, and transferred into new tubes in which the exosomes were lysed by incubating in 25 µL of radioimmunoprecipitation assay (RIPA) buffer (Thermo-Fisher Scientific) containing PPI for 10 min at room temperature and stored at – 80 °C.

### On-bead flow-cytometry analysis of CD9+ exosome complexes

EVs precipitated from pooled human serum by the ExoQuick kit were resuspended in 1% (w/v) BSA in PBS and incubated with magnetic beads conjugated to anti-L1CAM

or anti-MOG antibodies, as described above. As a negative control, the same beads were incubated with 1% (w/v) BSA in PBS in the absence of exosomes. After the incubation, the beads were washed twice in cold PBS and resuspended in 200 µL of exosome-stain buffer (system Biosciences). Five microliters of FITC-conjugated anti-human CD9 antibody (clone SN4 C3 3A2, eBioscience, USA) were added and incubated for 2 h at 4 °C with gentle rotation. Following washing, the beads were resuspended in 500 µL of wash buffer (System Biosciences) and 5000 events were counted using a BD LSR II flow-cytometry instrument (BD Biosciences, USA). The data were analyzed using FlowJo software.

### Microfluidic resistive pulse sensing

MRPS measurements were performed using an nCS1 instrument (Spectradyne, USA) equipped with disposable TS-300 polydimethylsiloxane cartridges. To generate an appropriate ionic electrical current in the analyte, 1% (w/v) BSA in PBS, pH 7.4, was used as a running buffer. Three µL of sample were used for measurement and ≥ 1000 particles were counted per analysis. Calibration was performed using calibration beads and data were analyzed using nCS1 Data Analyzer (Spectradyne). Filters were applied for data analysis to exclude false-positive signals. The filters excluded detected particle events characterized by user-defined signal-to-noise ratio, transit time, particle diameter or peak symmetry.

### TEM analysis of immunoprecipitated exosomes

Exosomes were eluted from anti-L1CAM- or anti-MOG-coated beads using 50 µL of exosome-elution buffer (System Biosciences), mixed with 50 µL 2% (v/v) paraformaldehyde (PFA) in PBS, and incubated for 20 min. Formvar carbon-coated grids (FCF400-CU, Electron Microscopy Sciences) were glow-discharged on a Pelco easiGlow instrument (Ted Pella, Inc.) for 2 min. Twenty µL of the fixed-exosome solution were placed on the grid and incubated for 20 min at RT. The grids then were washed thrice by floating them upside down on a 100-µL drop of filtered, deionized water (Milli-Q, Millipore). Exosomes were further fixed on the grids in 20 µL of 1% (v/v) glutaraldehyde for 5 min and stained with 2% (w/v) uranyl acetate for 10 min. The grids were washed twice in deionized water and imaged using a JEOL JEM-1200 EX transmission electron microscope operated at an acceleration voltage of 80 kV at a magnification of 80,000×.

### ECLIA measurement of α-syn

α-Syn concentration was measured using a U-PLEX Human α-Synuclein Kit (Meso Scale Discovery) according to the manufacturer's instructions. The measurements were done

by users blinded to diagnosis, demographic data, or any other identifying information. Briefly, a biotinylated anti-human  $\alpha$ -syn capture antibody was added to small-spot streptavidin-coated wells and incubated at room temperature with shaking at 800 rpm for 1 h. After washing the wells thrice with PBS containing 0.5% (v/v) Tween-20, samples and calibration standards were added along with a Sulfo-TAG-conjugated anti-human  $\alpha$ -syn detection antibody and incubated at room temperature with shaking at 800 rpm for 2 h. After washing the wells thrice, read buffer was added and the plates were read using MSD Sector Imager (Model-1250) or QuickPlex SQ 120 instruments. The data were analyzed using Discovery Workbench 4.0 software and quantified with reference to a freshly prepared  $\alpha$ -syn standard curve.

### Analysis of L1CAM in fractionated serum/plasma

Size-exclusion columns (35 nm, qEVoriginal, Izon sciences) were used to fractionate pooled serum or plasma samples (Innovative Research, Novi, MI). According to the manufacturer's instructions, exosomes elute in fractions 6–10, whereas fractions 11–17 contain free proteins and other smaller molecules in the serum/plasma. The eluted fractions were analyzed using an L1CAM ELISA kit (Millipore-Sigma, St. Louis, MO) according to manufacturer's instructions. Briefly, the samples and human L1CAM protein standards were added to the capture-antibody-coated wells and incubated for 2.5 h at room temperature. After washing the wells four times, biotinylated anti-L1CAM detection antibody was added to the wells and incubated for 1 h. Wells then were washed four times and incubated with HRP-conjugated streptavidin for 45 min at room temperature with gentle agitation. After washing the wells, TMB substrate was added and further incubated for 30 min in the dark with gentle agitation. Finally, a stop solution was added and the wells were read at 450 nm immediately.

### Statistical analysis

For all descriptive analyses, categorical variables were expressed as frequency (percentage), whereas continuous variables were expressed as median (interquartile range). Baseline variables were compared between the training and the validation cohorts separately for each group using the Chi-square or Fisher's tests for comparisons involving categorical variables and the Wilcoxon rank sum test for comparisons involving continuous variables. Each of the individual biomarkers were compared across groups using the Kruskal–Wallis test. Correlations across individual biomarkers were evaluated using the Spearman method. Multivariable models for predicting diagnosis status based

on multiple biomarkers combined were developed in the discovery cohort dataset using the multinomial logistic model with LASSO variable selection. Prediction accuracy for each pairwise combination of groups was performed using receiver-operating characteristic (ROC) analysis based on the above logistic model in the discovery cohort and in the validation cohort. Reported are the area under the curve (AUC), the sensitivity, and the specificity, which were evaluated at the best threshold, defined as the value of the linear predictor in the logistic model which maximized the unweighted sum of the sensitivity and the specificity. Multivariable analyses were performed using four additional classifiers including the linear discriminant analysis [11], quadratic discriminant analysis [11], classification tree for binary recursive partitioning [9], and K-nearest neighbor [42]. The prediction accuracies of each model were evaluated using the method by Hand and Till [26]. For the PD and MSA groups, probable vs possible diagnosis, and for MSA-C vs MSA-P, biomarkers were compared using the Wilcoxon rank sum test. The correlation between individual biomarkers and clinical measures of progression were evaluated using the Spearman method. The associations between selected measures of progression and multiple biomarkers combined were evaluated using linear regression models as sample size permitted. Analyses were performed using Prism 8.4 (GraphPad, San Diego, CA) or R version 4.0.2 (Copyright © 2020 The R Foundation for Statistical Computing).

## Results

### Inclusion strategy

Unlike biomarker studies that emphasize strict control of sample collection protocols and matching among groups and cohorts, we used more lenient inclusion criteria in an attempt to obtain a better representation of the high variability in the patient population and in various clinical settings. Both the discovery and validation cohorts included samples collected either in the field in a population-based study or in university-hospital-based clinics. Patients with PD were characterized by the diagnosing specialists as definite, probable, or possible PD and patients with MSA included both probable and possible diagnosis. In each MSA category, both the cerebellar type (MSA-C) and parkinsonian type (MSA-P) were included. In the discovery cohort, all the samples were serum, whereas in the validation cohort, ~40% of the samples were plasma.

A detailed description of the exosome isolation, enrichment, origin validation, assay reproducibility, and

limitation of sample storage period is provided as Supplementary Results and Supplementary figs. 1–5, online resources.

## Discovery cohort

Before immunoprecipitation of exosomes using CNS biomarkers, we asked whether the total number of exosomes or the total concentration of  $\alpha$ -syn in the serum samples differed among the groups. The number of exosomes can be estimated conveniently using a commercial CD81 ELISA kit in which the CD81 signal is converted to exosome concentration. To improve normalization of the data for statistical analysis, here and in all subsequent analyses, the values were log-transformed and are presented as log values in the figures. However, the untransformed values are discussed in the text to facilitate comparison with other studies.

The analysis showed a decrease in exosome concentration from  $4.4 \times 10^{10} \pm 3.1 \times 10^{10}$  exosomes per mL in the control group to  $3.7 \times 10^{10} \pm 3.6 \times 10^{10}$  and  $3.1 \times 10^{10} \pm 3.4 \times 10^{10}$  in the PD and MSA groups, respectively (Supplementary Fig. 6a, online resource). Although these differences were statistically insignificant, because the same trend was found in the validation cohort, the exosome concentration was included in the final multivariate statistical model used to separate the groups (see below). The exosome concentrations did not correlate with disease duration in either group. Measurement of serum  $\alpha$ -syn showed insignificant differences among the groups (Supplementary Fig. 6b, online resource).

In both the putative neuronal and oligodendroglial exosomes,  $\alpha$ -syn increased in the order control < PD < MSA (Fig. 1a). The  $\alpha$ -syn concentrations in the PD group (putative neuronal  $107 \pm 124$  pg/mL, putative oligodendroglial  $81 \pm 104$  pg/mL) were significantly higher than in the control (putative neuronal  $58 \pm 55$  pg/mL, putative oligodendroglial  $53 \pm 73$  pg/mL) and significantly lower than in the MSA group (putative neuronal  $191 \pm 131$  pg/mL, putative oligodendroglial  $286 \pm 348$  pg/mL). Interestingly, these results contradicted the observations of Jiang et al. [32] and Yu et al. [70] who reported lower  $\alpha$ -syn concentrations in putative CNS-originating exosomes from patients with MSA compared to those with PD.

To evaluate the degree of overlap among the groups, we used ROC analyses. The separation between the control and PD groups was low in both the putative neuronal (AUC = 0.674, Fig. 1b) and putative oligodendroglial (AUC = 0.628, Fig. 1c) exosomes, in agreement with results reported previously by Shi et al. (AUC = 0.654 in putative neuronal exosomes from 215 control and 267 PD plasma samples) [61]. In contrast, high separation was found between the control and MSA groups, particularly in the putative oligodendroglial exosomes (AUC = 0.924, Fig. 1c).

$\alpha$ -Syn concentration in putative oligodendroglial exosomes also provided better separation between the PD and MSA groups (AUC = 0.867, Fig. 1c) than in putative neuronal exosomes (AUC = 0.769, Fig. 1b).

> 90% of the samples in the control and PD groups were from the UCLA PEG study in this cohort, precluding meaningful testing of a source effect. In the MSA group, 21 samples were from UCLA and 9 from NYU. Comparing the putative neuronal and oligodendroglial  $\alpha$ -syn concentrations in the samples from these two sources we found in both cases that the concentrations in the NYU samples were significantly higher (Supplementary Table 1, online resource).

## The oligodendroglial: neuronal exosomal $\alpha$ -syn ratio improves the separation of PD from MSA

We asked next whether the known preference for deposition of  $\alpha$ -syn in neurons in PD versus oligodendrocytes in MSA could further help distinguish between these groups, even though the measurement in our assay was of total, rather than aggregated  $\alpha$ -syn. In agreement with the pattern of pathological  $\alpha$ -syn deposition in the brain, in the PD group, the average  $\alpha$ -syn concentration in the putative neuronal exosomes was higher than in the putative oligodendroglial exosomes, whereas the opposite was true in the MSA group (Fig. 1a). Therefore, we calculated the ratio between the  $\alpha$ -syn concentration in the putative oligodendroglial and putative neuronal exosomes (oligo:neuro ratio) for each sample (Fig. 2a). In most cases, the ratio was as expected, < 1 for PD and > 1 for MSA, yielding AUC = 0.916 (Fig. 2b), corresponding to 90.0% sensitivity and 88.2% specificity. Importantly, unlike the total  $\alpha$ -syn concentrations that differed significantly between the UCLA and NYU MSA samples, the difference between the average ratio values was insignificant (Supplementary Table 1, online resource), suggesting that the ratio may serve to remove variations among collection sites.

## Validation cohort

The samples used in our discovery cohort were collected from patients diagnosed clinically and not validated pathologically. To our knowledge, serum or plasma samples collected from living patients whose brains were analyzed pathologically after death are not available in sufficient numbers in any current biobank, especially considering that the samples cannot be > 5 years in storage. Therefore, we attempted to use samples collected post-mortem with a short post-mortem interval (PMI) from patients whose diagnosis was validated pathologically. Unfortunately, we found that in such samples, erythrocyte  $\alpha$ -syn contaminated the signal and did not allow meaningful analysis of  $\alpha$ -syn in putative CNS-originating exosomes (Supplementary Results,

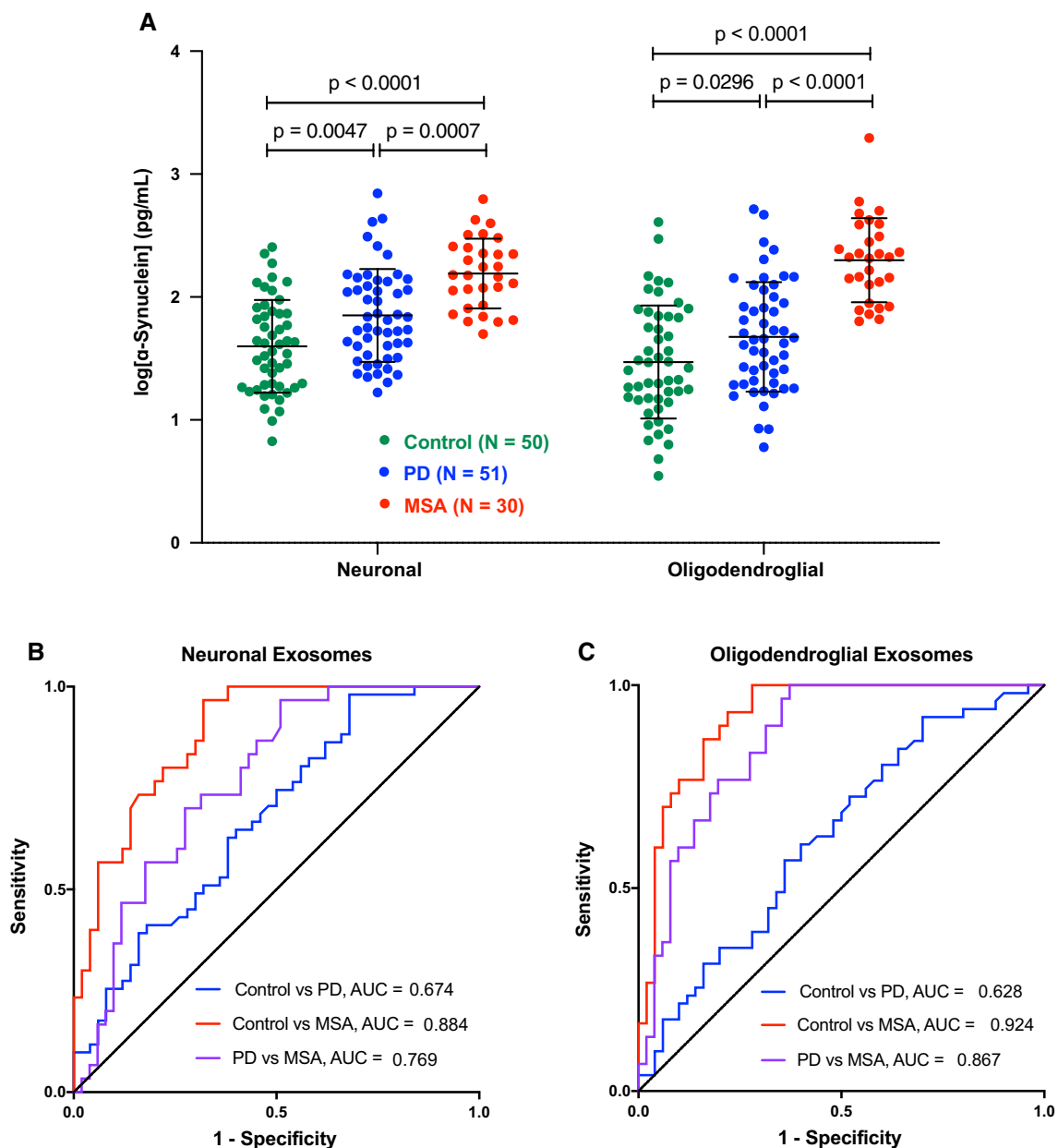


**Fig. 1** α-Syn concentration in putative neuronal and oligodendroglial exosomes differs significantly among the groups in the discovery cohort. **a** α-Syn concentrations were measured using ECLIA, log-transformed, and analyzed by a two-way ANOVA with post hoc

Tukey test. The data are presented as mean ± SD. **b** ROC analyses of α-syn concentration in putative neuronal exosomes. **c** ROC analyses of α-syn concentration in putative oligodendroglial exosomes

Supplementary Table 2, and Supplementary figs. 7, 8, online resources).

In the absence of pathologically validated samples, we obtained next a new set of samples to assemble a validation cohort. Most of these samples were obtained again from the UCLA PEG study (control and PD), the UCLA Clinical Neurogenomics Research Center (MSA), and the NYU Dysautonomia Center (PD and MSA). An additional major source of samples for this cohort was a biobank at

Columbia University (control and MSA). Comparison of the two cohorts showed that the groups did not differ significantly in their composition in terms of sex, ethnicity, and age (Supplementary Table 3, online resource). A few samples from the UCLA Easton Center were included originally but later eliminated, because their storage time was > 5 years. Because this cohort contained both serum and plasma samples, an adjustment of the raw data was necessary to allow

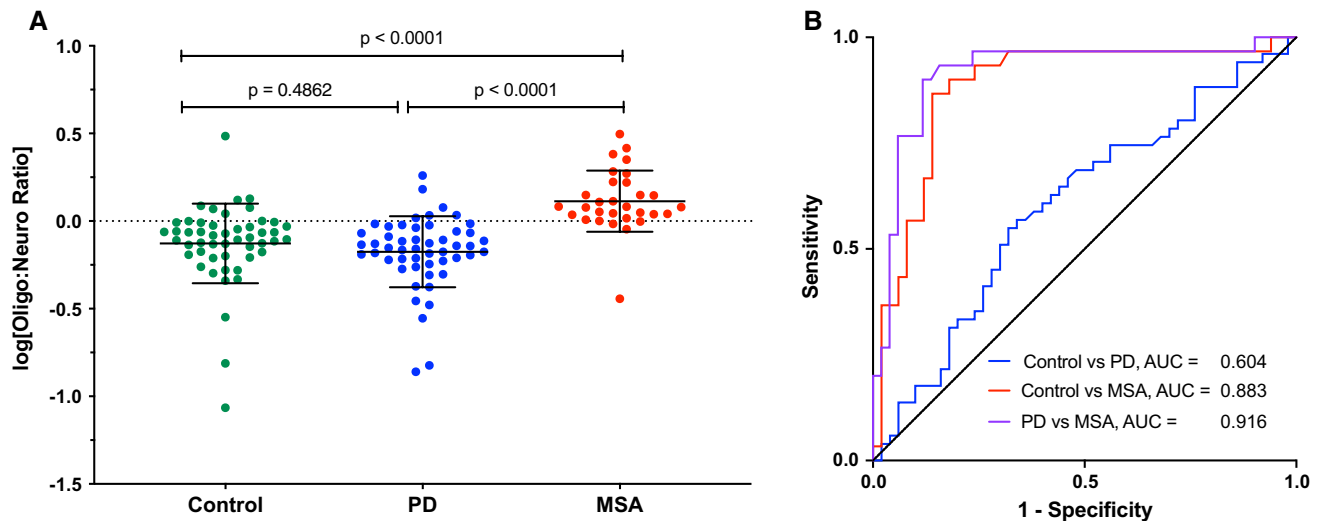


**Fig. 2** The ratio between  $\alpha$ -syn concentrations in putative oligodendroglial and neuronal exosomes improves the separation between PD and MSA. **a** The ratio between the  $\alpha$ -syn concentration in putative oligodendroglial and neuronal exosomes was calculated for each sam-

ple and log-transformed. The data are presented as mean  $\pm$  SD. The dashed line indicates the cutoff at 0 (log1). *P* values were calculated using a one-way ANOVA with post hoc Tukey test. **b** ROC analysis of the oligodendroglial:neuronal  $\alpha$ -syn ratio

analysis of these samples together (Supplementary Results and Supplementary Fig. 9, online resources).

Similar to the discovery cohort, before immunoprecipitation, there was a trend toward reduced exosome concentration in the serum/plasma samples in the order: control > PD > MSA (Supplementary Fig. 10a, online resource). Interestingly, unlike the discovery cohort,  $\alpha$ -syn concentration in the serum/plasma was substantially higher in the MSA group ( $486 \pm 479$  pg/mL) than in the control ( $187 \pm 241$  pg/mL) or PD ( $208 \pm 183$  pg/mL) groups (Supplementary Fig. 10b, online resource). As the majority of the MSA samples in this group were from Columbia University, we asked if differences among the sample sources might have accounted for the higher serum/plasma  $\alpha$ -syn levels in this cohort. Comparison among the sources showed that despite the larger number of samples from Columbia University, the variability in these samples was lower than in the samples from UCLA or NYU, yet the differences among the groups were statistically insignificant (Supplementary Fig. 10c, online resource). The increased  $\alpha$ -syn concentration in the MSA group could be partially attributed to the differences between the serum and adjusted plasma concentrations in these samples (Supplementary Fig. 9c, online resource). In addition, there was a larger fraction of MSA-P in the validation cohort (33.3%, including 4 samples with a mixed MSA-P/MSA-C diagnosis) compared to the discovery cohort (13.3%). On average, samples from patients diagnosed with MSA-C had lower serum/plasma  $\alpha$ -syn concentrations ( $353 \pm 251$  pg/mL) than samples from patients with MSA-P or mixed diagnosis ( $547 \pm 669$ ,  $p = 0.062$ , Student's *t* test). Thus, the larger fraction of the latter in the validation

cohort possibly also contributed to the increased concentration of serum/plasma  $\alpha$ -syn in this cohort's MSA group.

Similar to the discovery cohort, the  $\alpha$ -syn concentrations increased in the order: control < PD < MSA in both the putative neuronal and oligodendroglial exosomes, though the difference between the control and PD groups was statistically significant only for the latter (Fig. 3a). Higher concentrations of  $\alpha$ -syn were observed in the immunoprecipitated exosomes from the MSA group in this cohort, possibly for the same reasons discussed above for serum/plasma  $\alpha$ -syn. The average  $\alpha$ -syn concentration in the PD group (putative neuronal  $110 \pm 136$  pg/mL, putative oligodendroglial  $96 \pm 148$  pg/mL) was closer to the control group (putative neuronal  $96 \pm 110$  pg/mL, putative oligodendroglial  $60 \pm 91$  pg/mL) and substantially lower than the MSA group (putative neuronal  $284 \pm 251$  pg/mL, putative oligodendroglial  $497 \pm 360$  pg/mL). Accordingly, the separation between the control and PD groups was moderate in both the putative neuronal (AUC = 0.611, Fig. 3b) and putative oligodendroglial (AUC = 0.645, Fig. 3c) exosomes, whereas the separation between the control and MSA groups, particularly in the putative oligodendroglial exosomes was high (AUC = 0.947, Fig. 3c).  $\alpha$ -Syn concentration in putative oligodendroglial exosomes provided better separation between the PD and MSA groups (AUC = 0.920, Fig. 3c) than in putative neuronal exosomes (AUC = 0.824, Fig. 3b), mirroring the discovery cohort.

Analysis of the oligo:neuro ratio (Fig. 4a) showed that the number of PD samples for which the ratio was < 1 was lower in this cohort (69.8%) than in the discovery cohort (88.2%), whereas the fraction of MSA samples for



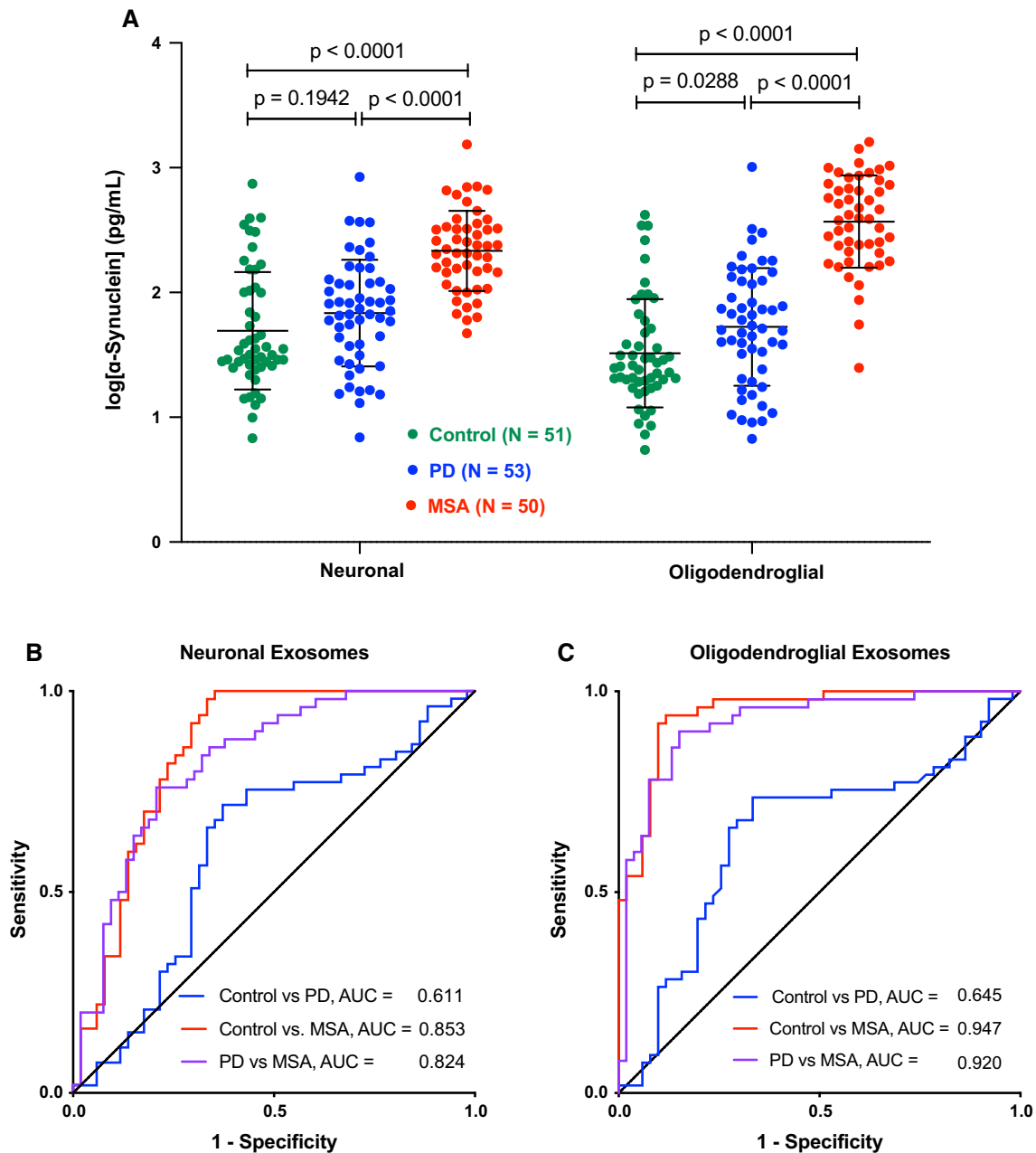


**Fig. 3** α-Syn concentration in putative neuronal and oligodendroglial exosomes differs among the groups in the validation cohort. **a** α-Syn concentrations were measured using ECLIA, log-transformed, and analyzed by a two-way ANOVA with post hoc Tukey test. The data

are presented as mean ± SD. **b** ROC analyses of α-syn concentration in putative neuronal exosomes. **c** ROC analyses of α-syn concentration in putative oligodendroglial exosomes

which the ratio was > 1 was similar in the validation cohort (90.0%) to the discovery cohort (86.7%). Accordingly, the separation between the PD and MSA groups was somewhat lower in the validation cohort, AUC = 0.871.

### Multivariable models for separation between PD and MSA

To further explore the degree to which the measured biomarkers could help improve distinguishing between PD and MSA, we tested several statistical models, including: (1) a multinomial logistic model with LASSO variable selection [16, 64]; (2) a linear discriminant model; (3) a classification

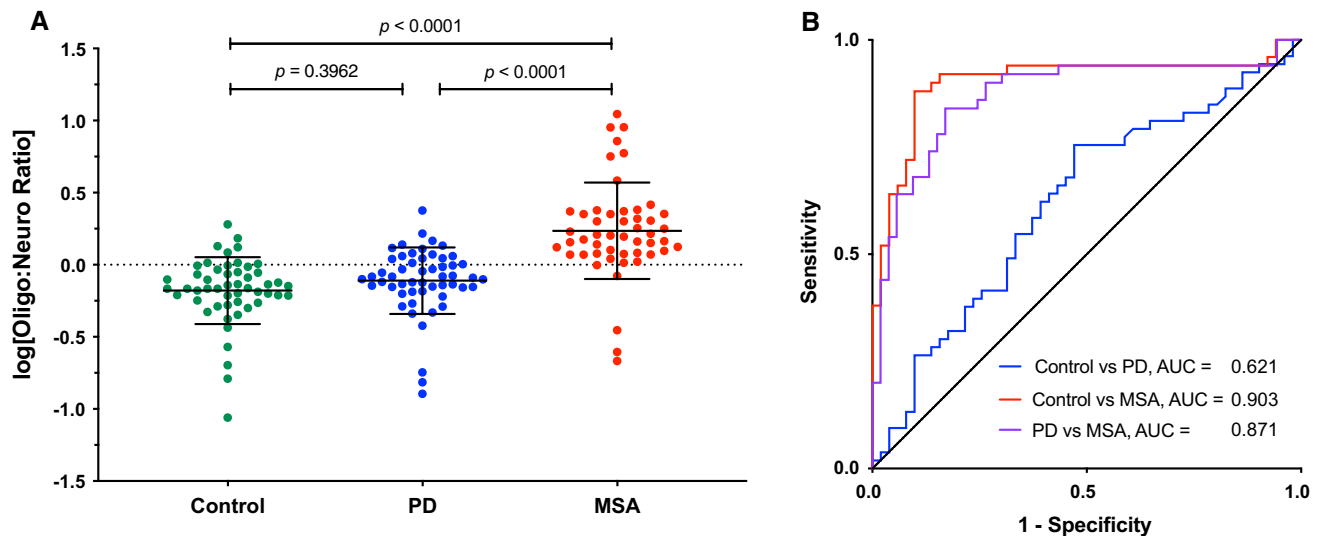


**Fig. 4** Validation of the separation between PD and MSA by the ratio between  $\alpha$ -syn concentrations in putative oligodendroglial and neuronal exosomes. **a** The ratio between the  $\alpha$ -syn concentration in putative oligodendroglial and neuronal exosomes was calculated for each

sample and log-transformed. The data are presented as mean  $\pm$  SD. The dashed line indicates the cutoff at 0 (log1). *P* values were calculated using a one-way ANOVA with post hoc Tukey test. **b** ROC analysis of the oligodendroglial:neuronal exosome  $\alpha$ -syn ratio

tree model; and (4) a K-nearest-neighbor model. In each case, the model was trained on the discovery cohort and was challenged with selecting among the putative neuronal exosomal  $\alpha$ -syn, putative oligodendroglial exosomal  $\alpha$ -syn, oligo:neuro ratio, and serum/plasma exosome concentration of the combination providing the best separation among the groups in a ROC analysis. Because the first three parameters are interdependent, the models were expected to select two out of the three and fulfilled this expectation in all cases. The formula created by the model then was applied to the validation cohort to test to what extent the discrimination power could be reproduced.

All the models, except the K-nearest-neighbor model, which yielded poor accuracy (data not shown), provided similar results (Supplementary Table 4, online resource), yet the multinomial logistic model yielded the highest discrimination power. The model selected the putative neuronal exosomal  $\alpha$ -syn, oligo:neuro ratio, and serum/plasma exosome concentration to create the discriminative formula, which in the discovery cohort separated the control and PD groups with AUC=0.762, control and MSA with AUC=0.961, and PD and MSA groups with AUC=0.928. When the formula created by the model was applied to the validation cohort, it separated the control and PD groups with AUC=0.610, control and MSA with AUC=0.962, and PD and MSA groups with AUC=0.902, corresponding to 89.8% sensitivity and 86.0% specificity.

A limitation of our study's design was that it did not emphasize inclusion of early stage patients, in which the potential for misdiagnosis is highest. Most patients with PD in our study were 5–8 years from diagnosis, whereas

the disease duration in the MSA group was mostly 3–5 years (Supplementary Fig. 11a, online resource). Examination of the biomarkers reported here in patients with early stage disease will be pursued in the future. Nonetheless, to test whether the main biomarker, the oligo:neuro ratio, can be detected in early stage disease or only develops at later stages, we tested whether this biomarker correlated with disease duration. Spearman analysis showed that the oligo:neuro ratio did not correlate with disease duration (Supplementary Fig. 11b–e, online resource), suggesting that it could be a useful biomarker already at the time of diagnosis.

Another potential limitation of the study is that the reference used for biomarker accuracy is the clinical diagnosis, which as discussed in the Introduction, is prone to error. Though validation of the biomarker's accuracy through a neuropathological examination was not possible in most cases, toward the end of the study, we went back and checked whether any clinical diagnosis was validated after patients passed away or changed by the diagnosing clinicians. The data are presented in Supplementary Table 5 (online resource).

In the PD groups (both cohorts combined), one diagnosis was changed from PD to MSA-P, which was predicted correctly by the model. Two patients' diagnosis was changed from PD to Parkinson's disease dementia (PDD), of which one was predicted by the model to be MSA. No diagnosis was pathologically validated in this group. In the MSA group, the model predicted correctly the diagnosis of 11 out of 13 patients whose diagnosis with MSA, or in two cases MSA mixed with AD, was confirmed pathologically.

In two cases, both of which were diagnosed clinically with probable MSA-C and later validated pathologically as MSA, the model predicted incorrectly a diagnosis of PD. These numbers are in agreement with the degree of sensitivity and specificity of the model described above.

In contrast to the diagnostic power of the biomarkers we measured, we did not find cross-sectional correlation with disease severity for any of the biomarkers, including measurements of motor deterioration (UPDRS-III, UMSARS, H&Y) or cognitive function (MMSE).

## Discussion

A diagnostic test for synucleinopathies is an urgent unmet medical need both for currently available treatments and for stratifying patients in clinical trials of new therapies. A blood-based test offers several advantages over current methodologies. It can be performed in typical clinics, does not require the use of radionuclides in the brain or a lumbar puncture, and is cost-effective. Analysis of biomarkers in CNS-originating exosomes allows comparison among exosomes from different cell types, offering an additional advantage compared to CSF analysis. Thus, for distinguishing between PD and MSA, we found that the ratio between  $\alpha$ -syn concentration levels in putative oligodendroglial and neuronal exosomes was particularly useful, as most patients with PD were found to have higher  $\alpha$ -syn levels in their putative neuronal exosomes, whereas those with MSA had higher levels in putative oligodendroglial exosomes, providing AUC = 0.871–0.916 in ROC analyses (Figs. 2, 4). In addition, the  $\alpha$ -syn concentration in putative oligodendroglial exosomes itself was useful for separating the MSA from both the control and PD groups, in agreement with the lack of expression of  $\alpha$ -syn in normal mature oligodendrocytes. The putative oligodendroglial exosomal  $\alpha$ -syn concentration was significantly higher in MSA than in PD and separated between the PD and MSA groups with AUC = 0.867–0.920 (Figs. 1, 3). This result was in agreement with analyses of total brain  $\alpha$ -syn, which showed that the concentrations, particularly in membrane-associated and insoluble extracts, are higher in MSA than in PD brains [58, 65].

Our study used methodologies first introduced by Shi et al. in PD research [61] and Goetzl and co-workers in the AD field [17], who used L1CAM to immunoprecipitate putative neuronal exosomes from serum or plasma. The high level of separation we achieved between the PD and MSA groups was facilitated by adding to this methodology immunoprecipitation of putative oligodendroglial exosomes using the specific oligodendrocyte marker MOG. We chose MOG, because it is a membrane-bound protein [7] and because specific commercial antibodies are available against its extracellular domain, which we

predicted might be exposed on the surface of exosomes. Recently, Yu et al. have analyzed  $\alpha$ -syn concentrations in putative oligodendroglial exosomes immunoprecipitated from plasma of patients with PD or MSA using a different oligodendrocyte marker, CNPase, and reported lower  $\alpha$ -syn concentrations in the MSA groups compared to PD [70], in contrast to our findings (Figs. 1, 3). Although there are several methodological differences between the study by Yu et al. and our report, the most likely explanation for the apparent discrepancy in the results is the difference in the markers used for immunoprecipitating the exosomes. Although both MOG and CNPase are membrane-bound proteins expressed specifically by oligodendrocytes, CNPase is present on the cytosolic side of non-compact myelin [14, 66] and the intermembrane space of mitochondria [37], which may limit its presentation on the surface of exosomes. An alternative explanation is differences in the antibodies used for  $\alpha$ -syn quantitation in the different studies. MSD does not share the identity of the capture and detection antibodies in the ECLIA kit we used, precluding making a side-by-side comparison.

Several other recent studies have reported biomarkers that could help distinguish between PD and MSA. Hansson et al. measured neurofilament light chain (NfL) in blood and CSF samples from patients with PD and other parkinsonian disorders, including PSP, corticobasal degeneration (CBD), and MSA [28] obtained from three different cohorts. As has been reported now in multiple studies [22, 43], a strong correlation was found between blood and CSF levels of NfL. NfL concentrations were elevated in PSP, CBD, and MSA compared to PD and healthy controls, allowing separation of the PD and MSA groups with AUC = 0.81–0.91 in the different cohorts [28]. PSP, CBD, and MSA samples had comparable levels of NfL. As PSP and CBD are tauopathies,  $\alpha$ -syn levels in neuronal and oligodendroglial exosomes in these diseases are expected to be substantially lower than in MSA. Therefore, combining blood NfL with CNS-exosomal  $\alpha$ -syn could allow separating MSA not only from PD but also from PSP and CBD.

More recently, Jiang et al. have reported that  $\alpha$ -syn in putative neuronal exosomes isolated from the serum of patients with PD and several atypical parkinsonian syndromes was a useful diagnostic biomarker [32]. Although similar to most studies in this field, L1CAM was used for immunoprecipitation of the exosomes, they used a distinct kind of polymeric support from the one used by most groups, in an attempt to decrease non-specific binding of the exosomes to the beads themselves. They reported that  $\alpha$ -syn concentrations in the putative neuronal exosomes from PD samples were higher than in MSA samples, in contrast to our findings. Although their study also included three cohorts, MSA samples were available in only one and their number was limited to 14 [32]. As with the study by Yu et al.,

the most likely explanation for the difference between their results and ours is the use of different reagents for immunoprecipitation. An important discovery in the study by Jiang et al. was that in addition to  $\alpha$ -syn, clusterin concentrations in the putative neuronal exosomes also differed substantially among the disease groups. The combination of  $\alpha$ -syn and clusterin allowed separating the small MSA group from the counterpart PD group with AUC = 0.94. This important discovery suggests that clusterin should be included in future studies aimed at validating these initial results.

An important recent study by Shah Nawaz et al. found that PD and MSA could be separated with an overall sensitivity of 95.4% by applying protein misfolding cyclic amplification (PMCA) to CSF samples from 94 patients with PD and 75 patients with MSA (clinical diagnosis in all cases) [59]. The PMCA technique allows measurement of fibrillar  $\alpha$ -syn with high sensitivity by signal amplification. Moreover, this and other studies (e.g., by Prusiner et al. [54]) have demonstrated that  $\alpha$ -syn fibrils in PD and MSA form distinct conformational strains. Although our ECLIA measurements were of total  $\alpha$ -syn, we cannot rule out that some of the differences we observed might have stemmed from different antibody reactivity toward  $\alpha$ -syn strains in the PD and MSA samples. Future studies will tell if PMCA or similar techniques can be applied to  $\alpha$ -syn in CNS-originating exosomes, which would alleviate the need for a lumbar puncture and offer the advantage of analyzing fibrillar  $\alpha$ -syn in exosomes from different cell types, as was done here.

Though > 50 studies have demonstrated the utility of analyzing putative CNS-originating exosomes as a source of biomarkers to date, the ability to use anti-L1CAM antibodies for enriching putative neuronal exosomes by immunoprecipitation recently has come under scrutiny due to the existence of multiple forms of the protein, both soluble and membrane-bound, and because L1CAM is expressed also outside the brain in non-neuronal cells [47]. It is widely acknowledged that immunoprecipitation using L1CAM is expected to enrich CNS-neuronal exosomes, rather than to yield a pure population. Our data demonstrate the existence of small amounts of L1CAM in SEC fractions containing exosomes by the same method used by Norman et al. [47] (Supplementary Fig. 3, online resource). We also did not find high non-specific binding of  $\alpha$ -syn to beads conjugated to the anti-L1CAM antibody 5G3 as found by Norman et al. for antibody UJ127. Our data strongly suggest that L1CAM is present on the surface of neuronal exosomes and can be used to immunoprecipitate CNS-neuronal exosomes. Nonetheless, as L1CAM is also expressed by other tissues and low levels of MOG RNA also have been reported in non-CNS cells, a presence of  $\alpha$ -syn in exosomes immunoprecipitated using these two markers but originating outside the CNS could contribute to the data we observed. Such contribution would be expected to be different for PD, where peripheral

$\alpha$ -syn deposition in the enteric system and the skin has been reported, and MSA, in which  $\alpha$ -syn accumulation is thought to be limited to the CNS.

To our knowledge, a limitation of all the studies published to date using the strategy of biomarker analysis in putative CNS-originating exosomes, including our study, is the lack of validation of the cellular origin of the exosomes. We made multiple attempts to analyze potential markers, other than those used for immunoprecipitation, to validate the neuronal or oligodendroglial origin of the exosomes in our study, yet due to the very limited amounts of immunoprecipitated exosomes, the results were inconsistent. Future studies, likely using highly sensitive techniques, such as ECLIA or single-molecule array (Simoa), will be needed to achieve reliable validation of exosome origin.

Because MSA is a rare disease, obtaining large numbers of biofluid samples is challenging. Collection of samples from several sources, particularly in the case of MSA, limited the availability of consistent clinical measures. For example, clinics specializing in movement disorders or autonomic failure used the more common UMSARS scale to measure disease progression, whereas the ataxia-focused clinics used the SARA scale, limiting the ability to compare among these datasets. For cognitive evaluation, some of the providing clinics used the MMSE test, whereas others used MoCA. Although we converted the MoCA score to MMSE [36], these differences might have compromised our ability to obtain meaningful correlation between the biomarkers and cognitive decline, though a more likely explanation for the lack of correlation we observed was the fact that most of the samples were from patients with little or no cognitive decline.

We combined samples from several sources to obtain two independent cohorts that would allow validating the predictions made using the discovery cohort in the independent validation cohort. A conscious decision we made was to use relatively lenient inclusion criteria in anticipation of high heterogeneity not only in the patient population, but also among clinics and biobanks providing the samples, a prediction that proved to be correct (Supplementary Table 1, online resource). With these considerations in mind, we conducted extensive quality control experiments to ensure that the included samples reflected *bona fide*  $\alpha$ -syn in putative CNS exosomes and that technical parameters, such as storage time or number of freeze–thaw cycles would not affect the final measurement. Although the diagnosis was validated pathologically only in a small number of cases (Supplementary Table 5, online resource), our data demonstrate that even in a heterogeneous collection of samples, disease stages, and disease types (e.g., MSA-C vs MSA-P), the model based on the objective biomarkers we measured corresponded to the clinical diagnosis of approximately

nine out of ten patients in the PD and MSA groups. The diagnostic power was even higher for separating patients with MSA from healthy controls, whereas the separation of patients with PD from healthy individuals was moderate, as reported previously [61]. In the future, adding biomarkers, such as tau [60], pS129- $\alpha$ -syn [19, 35, 40, 69], and clusterin, and/or combining these biomarkers with measurements of oligomeric/aggregated  $\alpha$ -syn, as was demonstrated by Shah Nawaz et al. [59], holds promise for improving the diagnostic accuracy.

In conclusion, we tested and validated a blood-based diagnostic biomarker in two independent cohorts, which separates two related synucleinopathies, PD, and MSA, with high sensitivity and specificity. The biomarker is based on measurement of  $\alpha$ -syn concentrations in putative neuronal and oligodendroglial exosomes isolated from patients' serum or plasma. Additional validation in larger cohorts, and eventually in pathologically confirmed samples when those become available, may facilitate the use of this biomarker, potentially in combination with recently discovered ones, such as clusterin and fibrillar  $\alpha$ -syn, for routine clinical diagnosis of these diseases.

**Acknowledgements** We thank Dr. Greg Cole for the use of his MSD Imager. The work was supported by a generous gift from Team Parkinson/Parkinson Alliance (G.B.), a pilot grant from the UCLA American Parkinson's Disease Association Center (G.B.), NIH/NCRR UL1 TR000124 – UCLA Clinical and Translational Science Institute (CTSI) Voucher (G.B.), MSA Coalition grant 2017-10-007 (G.B.), California Department of Public Health grant 18-10926 (G.B.), The Alzheimer's Association, The Michael J. Fox Foundation, Weston Brain Institute, and Alzheimer's Research UK Biomarkers Across Neurodegenerative Diseases (BAND 3) grant 17990 (G.B.), CurePSP grant 665-2019-0 (G.B.), The Michael J. Fox Foundation grant 18303 (G.B.), a grant from the National Ataxia Foundation (G.B. and B.L.F.), NIH/NINDS grant U54NS065736 (H.K.), NIH/NINDS grant R01NS082094 (B.L.F.), and NIH/NIEHS grant ES10544 (B.R.). The Columbia University cohort is supported by the Parkinson's Foundation, the National Institutes of Health (K02NS080915 and UL1 TR000040), and the Brookdale Foundation. The Banner Sun Health Research Institute Brain and Body Donation Program of Sun City, Arizona, has been supported by the National Institute of Neurological Disorders and Stroke (U24 NS072026 National Brain and Tissue Resource for Parkinson's Disease and Related Disorders), the National Institute on Aging (P30 AG19610 Arizona Alzheimer's Disease Core Center), the Arizona Department of Health Services (contract 211002, Arizona Alzheimer's Research Center), the Arizona Biomedical Research Commission (contracts 4001, 0011, 05-901, and 1001 to the Arizona Parkinson's Disease Consortium), and the Michael J. Fox Foundation for Parkinson's Research.

**Author contributions** SD and GB conceptualized and designed the study and wrote the manuscript; SD, SH, AK, and KNM acquired the data; IdR, KCP, DM, SD, and GB analyzed the data; DW, ADF, JAP, GES, CHA, SLP, WWP, UJK, RNA, MS, KHG, HK, BLF, JMB, and BR provided samples and critical comments on the manuscript.

#### Declaration

**Conflict of interest** None of the authors has any financial disclosure or conflict of interest to report.

**Open Access** This article is licensed under a Creative Commons Attribution 4.0 International License, which permits use, sharing, adaptation, distribution and reproduction in any medium or format, as long as you give appropriate credit to the original author(s) and the source, provide a link to the Creative Commons licence, and indicate if changes were made. The images or other third party material in this article are included in the article's Creative Commons licence, unless indicated otherwise in a credit line to the material. If material is not included in the article's Creative Commons licence and your intended use is not permitted by statutory regulation or exceeds the permitted use, you will need to obtain permission directly from the copyright holder. To view a copy of this licence, visit <http://creativecommons.org/licenses/by/4.0/>.

## References

- Adler CH, Beach TG, Hentz JG, Shill HA, Caviness JN, Driver-Dunckley E et al (2014) Low clinical diagnostic accuracy of early vs advanced Parkinson disease: clinicopathologic study. *Neurology* 83:406–412. <https://doi.org/10.1212/WNL.0000000000000641>
- Alcalay RN, Levy OA, Waters CC, Fahn S, Ford B, Kuo SH et al (2015) Glucocerebrosidase activity in Parkinson's disease with and without GBA mutations. *Brain* 138:2648–2658. <https://doi.org/10.1093/brain/awv179>
- Alvarez-Erviti L, Seow Y, Schapira AH, Gardiner C, Sargent IL, Wood MJ et al (2011) Lysosomal dysfunction increases exosome-mediated  $\alpha$ -synuclein release and transmission. *Neurobiol Dis* 42:360–367. <https://doi.org/10.1016/j.nbd.2011.01.029>
- Beach TG, Adler CH (2018) Importance of low diagnostic accuracy for early Parkinson's disease. *Mov Disord* 33:1551–1554. <https://doi.org/10.1002/mds.27485>
- Beach TG, Adler CH, Sue LI, Serrano G, Shill HA, Walker DG et al (2015) Arizona study of aging and neurodegenerative disorders and brain and body donation program. *Neuropathology* 35:354–389. <https://doi.org/10.1111/neup.12189>
- Bellingham SA, Guo BB, Coleman BM, Hill AF (2012) Exosomes: vehicles for the transfer of toxic proteins associated with neurodegenerative diseases? *Front Physiol* 3:124. <https://doi.org/10.3389/fphys.2012.00124>
- Berger T, Reindl M (2007) Multiple sclerosis: disease biomarkers as indicated by pathophysiology. *J Neurol Sci* 259:21–26. <https://doi.org/10.1016/j.jns.2006.05.070>
- Beyer K, Ariza A (2007) Protein aggregation mechanisms in synucleinopathies: commonalities and differences. *J Neuropathol Exp Neurol* 66:965–974. <https://doi.org/10.1097/nen.0b013e3181587d64> (00005072-200711000-00001 [pii])
- Breiman L, Friedman J, Stone CJ, Olshen RA (1984) Classification and regression trees. CRC Press
- Brooks DJ, Seppi K, Neuroimaging Working Group on MSA (2009) Proposed neuroimaging criteria for the diagnosis of multiple system atrophy. *Mov Disord* 24:949–964. <https://doi.org/10.1002/mds.22413>
- Cover TM, Hart PE (1967) Nearest neighbor pattern classification. *IEEE Trans Inform Theory* 13:21. <https://doi.org/10.1109/Tit.1967.1053964>
- Danzer KM, Kranich LR, Ruf WP, Cagsal-Getkin O, Winslow AR, Zhu L et al (2012) Exosomal cell-to-cell transmission of  $\alpha$  synuclein oligomers. *Mol Neurodegener* 7:42. <https://doi.org/10.1186/1750-1326-7-42>




13. Desplats P, Lee HJ, Bae EJ, Patrick C, Rockenstein E, Crews L et al (2009) Inclusion formation and neuronal cell death through neuron-to-neuron transmission of  $\alpha$ -synuclein. *Proc Natl Acad Sci USA* 106:13010–13015. <https://doi.org/10.1073/pnas.0903691106> (0903691106 [pii])
14. Drummond GI, Perrott-Yee S (1961) Enzymatic hydrolysis of adenosine 3',5'-phosphoric acid. *J Biol Chem* 236:1126–1129
15. Emmanouilidou E, Melachroinou K, Roumeliotis T, Garbis SD, Ntzouni M, Margaritis LH et al (2010) Cell-produced  $\alpha$ -synuclein is secreted in a calcium-dependent manner by exosomes and impacts neuronal survival. *J Neurosci* 30:6838–6851. <https://doi.org/10.1523/JNEUROSCI.5699-09.2010>
16. Engel J (1988) Polytomous logistic regression. *Stat Neerl* 42:233–252
17. Fiandaca MS, Kapogiannis D, Mapstone M, Boxer A, Eitan E, Schwartz JB et al (2015) Identification of preclinical Alzheimer's disease by a profile of pathogenic proteins in neurally derived blood exosomes: a case-control study. *Alzheimers Dement* 11(600–607):e601. <https://doi.org/10.1016/j.jalz.2014.06.008>
18. Fogel BL, Clark MC, Geschwind DH (2014) The neurogenetics of atypical parkinsonian disorders. *Semin Neurol* 34:217–224. <https://doi.org/10.1055/s-0034-1381738>
19. Foulds PG, Diggle P, Mitchell JD, Parker A, Hasegawa M, Masuda-Suzukake M et al (2013) A longitudinal study on  $\alpha$ -synuclein in blood plasma as a biomarker for Parkinson's disease. *Sci Rep* 3:2540. <https://doi.org/10.1038/srep02540>
20. Frühbeis C, Fröhlich D, Krämer-Albers EM (2012) Emerging roles of exosomes in neuron-glia communication. *Front Physiol* 3:119. <https://doi.org/10.3389/fphys.2012.00119>
21. Frühbeis C, Fröhlich D, Kuo WP, Amphornrat J, Thilemann S, Saab AS et al (2013) Neurotransmitter-triggered transfer of exosomes mediates oligodendrocyte-neuron communication. *PLoS Biol* 11:e1001604. <https://doi.org/10.1371/journal.pbio.1001604>
22. Gaetani L, Blennow K, Calabresi P, Di Filippo M, Parnetti L, Zetterberg H (2019) Neurofilament light chain as a biomarker in neurological disorders. *J Neurol Neurosurg Psychiatry*. <https://doi.org/10.1136/jnnp-2018-320106>
23. Gilman S, Wenning GK, Low PA, Brooks DJ, Mathias CJ, Trojanowski JQ et al (2008) Second consensus statement on the diagnosis of multiple system atrophy. *Neurology* 71:670–676. <https://doi.org/10.1212/01.wnl.0000324625.00404.15>
24. Goetzl EJ, Boxer A, Schwartz JB, Abner EL, Petersen RC, Miller BL et al (2015) Altered lysosomal proteins in neural-derived plasma exosomes in preclinical Alzheimer disease. *Neurology* 85:40–47. <https://doi.org/10.1212/WNL.0000000000001702>
25. Goetzl EJ, Kapogiannis D, Schwartz JB, Lobach IV, Goetzl L, Abner EL et al (2016) Decreased synaptic proteins in neuronal exosomes of frontotemporal dementia and Alzheimer's disease. *FASEB J* 30:4141–4148. <https://doi.org/10.1096/fj.201600816R>
26. Hand DJ, Till RJ (2001) A simple generalisation of the area under the ROC curve for multiple class classification problems. *Mach Learn* 45:171–186. <https://doi.org/10.1023/A:1010920819831>
27. Hansen C, Angot E, Bergstrom AL, Steiner JA, Pieri L, Paul G et al (2011)  $\alpha$ -Synuclein propagates from mouse brain to grafted dopaminergic neurons and seeds aggregation in cultured human cells. *J Clin Invest* 121:715–725. <https://doi.org/10.1172/JCI43366>
28. Hansson O, Janelidze S, Hall S, Magdalino N, Lees AJ, Andreasson U et al (2017) Blood-based NfL: a biomarker for differential diagnosis of parkinsonian disorder. *Neurology* 88:930–937. <https://doi.org/10.1212/WNL.0000000000003680>
29. Hashimoto M, Masliah E (1999)  $\alpha$ -Synuclein in Lewy body disease and Alzheimer's disease. *Brain Pathol* 9:707–720
30. Hentz JG, Mehta SH, Shill HA, Driver-Dunckley E, Beach TG, Adler CH (2015) Simplified conversion method for unified Parkinson's disease rating scale motor examinations. *Mov Disord* 30:1967–1970. <https://doi.org/10.1002/mds.26435>
31. Hornung S, Dutta S, Bitan G (2020) CNS-derived blood exosomes as a promising source of biomarkers: opportunities and challenges. *Front Mol Neurosci* 13:38. <https://doi.org/10.3389/fnmol.2020.00038>
32. Jiang C, Hopfner F, Katsikoudi A, Hein R, Catli C, Evetts S et al (2020) Serum neuronal exosomes predict and differentiate Parkinson's disease from atypical parkinsonism. *J Neurol Neurosurg Psychiatry*. <https://doi.org/10.1136/jnnp-2019-322588>
33. Joutsa J, Gardberg M, Roytta M, Kaasinen V (2014) Diagnostic accuracy of parkinsonism syndromes by general neurologists. *Parkinsonism Relat Disord* 20:840–844. <https://doi.org/10.1016/j.parkreldis.2014.04.019>
34. Koga S, Aoki N, Uitti RJ, van Gerpen JA, Cheshire WP, Josephs KA et al (2015) When DLB, PD, and PSP masquerade as MSA: an autopsy study of 134 patients. *Neurology* 85:404–412. <https://doi.org/10.1212/WNL.0000000000001807>
35. Landeck N, Hall H, Ardah MT, Majbour NK, El-Agnaf OM, Halliday G et al (2016) A novel multiplex assay for simultaneous quantification of total and S129 phosphorylated human  $\alpha$ -synuclein. *Mol Neurodegener* 11:61. <https://doi.org/10.1186/s13024-016-0125-0>
36. Lawton M, Kasten M, May MT, Mollenhauer B, Schaumburg M, Liepelt-Scarfone I et al (2016) Validation of conversion between mini-mental state examination and montreal cognitive assessment. *Mov Disord* 31:593–596. <https://doi.org/10.1002/mds.26498>
37. Lee J, O'Neill RC, Park MW, Gravel M, Braun PE (2006) Mitochondrial localization of CNP2 is regulated by phosphorylation of the N-terminal targeting signal by PKC: implications of a mitochondrial function for CNP2 in glial and non-glial cells. *Mol Cell Neurosci* 31:446–462. <https://doi.org/10.1016/j.mcn.2005.10.017>
38. Leys F, Fanciulli A, Ndayisaba JP, Granata R, Struhal W, Wenning GK (2020) Cardiovascular autonomic function testing in multiple system atrophy and Parkinson's disease: an expert-based blinded evaluation. *Clin Auton Res* 30:255–263. <https://doi.org/10.1007/s10286-020-00691-4>
39. Lin J, Li J, Huang B, Liu J, Chen X, Chen XM et al (2015) Exosomes: novel biomarkers for clinical diagnosis. *Sci World J* 2015:657086. <https://doi.org/10.1155/2015/657086>
40. Majbour NK, Vaikath NN, van Dijk KD, Ardah MT, Varghese S, Vesterager LB et al (2016) Oligomeric and phosphorylated  $\alpha$ -synuclein as potential CSF biomarkers for Parkinson's disease. *Mol Neurodegener* 11:7. <https://doi.org/10.1186/s13024-016-0072-9>
41. McCann H, Stevens CH, Cartwright H, Halliday GM (2014)  $\alpha$ -Synucleinopathy phenotypes. *Parkinsonism Relat Disord* 20(Suppl 1):S62–67. [https://doi.org/10.1016/S1353-8020\(13\)70017-8](https://doi.org/10.1016/S1353-8020(13)70017-8)
42. McLachlan GJ (2004) Discriminant analysis and statistical pattern recognition. Wiley Interscience
43. Mielke MM, Syrjänen JA, Blennow K, Zetterberg H, Vemuri P, Skoog I et al (2019) Plasma and CSF neurofilament light: relation to longitudinal neuroimaging and cognitive measures. *Neurology* 93:e252–e260. <https://doi.org/10.1212/WNL.0000000000007767>
44. Mondello S, Buki A, Italiano D, Jeromin A (2013)  $\alpha$ -Synuclein in CSF of patients with severe traumatic brain injury. *Neurology* 80:1662–1668. <https://doi.org/10.1212/WNL.0b013e3182904d43>
45. Murray IVJ, Lee VMY, Trojanowski JQ (2001) Synucleinopathies: a pathological and molecular review. *Clin Neurosci Res* 1:445–455
46. Newman EJ, Breen K, Patterson J, Hadley DM, Grosset KA, Grosset DG (2009) Accuracy of Parkinson's disease diagnosis in 610

- general practice patients in the West of Scotland. *Mov Disord* 24:2379–2385. <https://doi.org/10.1002/mds.22829>
47. Norman M, Ter-Ovanesyan D, Trieu W, Lazarovitz R, Kowal EJK, Lee JH et al (2020) L1CAM is not associated with extracellular vesicles in human cerebrospinal fluid or plasma. *bioRxiv*. <https://doi.org/10.1101/2020.1108.1112.247833>
  48. Pahwa R, Lyons KE (2010) Early diagnosis of Parkinson's disease: recommendations from diagnostic clinical guidelines. *Am J Manag Care* 16(Suppl Implications):S94–S99
  49. Palermo G, Del Prete E, Bonuccelli U, Ceravolo R (2020) Early autonomic and cognitive dysfunction in PD, DLB and MSA: blurring the boundaries between  $\alpha$ -synucleinopathies. *J Neurol* 267:3444–3456. <https://doi.org/10.1007/s00415-020-09985-z>
  50. Palma JA, Norcliffe-Kaufmann L, Kaufmann H (2018) Diagnosis of multiple system atrophy. *Auton Neurosci* 211:15–25. <https://doi.org/10.1016/j.autneu.2017.10.007>
  51. Pellecchia MT, Stankovic I, Fanciulli A, Krismer F, Meissner WG, Palma JA et al (2020) Can autonomic testing and imaging contribute to the early diagnosis of multiple system atrophy? A systematic review and recommendations by the movement disorder society multiple system atrophy study group. *Mov Disord Clin Pract* 7:750–762. <https://doi.org/10.1002/mdc3.13052>
  52. Postuma RB, Berg D, Stern M, Poewe W, Olanow CW, Oertel W et al (2015) MDS clinical diagnostic criteria for Parkinson's disease. *Mov Disord* 30:1591–1601. <https://doi.org/10.1002/mds.26424>
  53. Properzi F, Logozzi M, Fais S (2013) Exosomes: the future of biomarkers in medicine. *Biomark Med* 7:769–778. <https://doi.org/10.2217/bmm.13.63>
  54. Prusiner SB, Woerman AL, Mordes DA, Watts JC, Rampersaud R, Berry DB et al (2015) Evidence for  $\alpha$ -synuclein prions causing multiple system atrophy in humans with parkinsonism. *Proc Natl Acad Sci USA* 112:E5308–5317. <https://doi.org/10.1073/pnas.1514475112>
  55. Rizzo G, Copetti M, Arcuti S, Martino D, Fontana A, Logroscino G (2016) Accuracy of clinical diagnosis of Parkinson disease: a systematic review and meta-analysis. *Neurology* 86:566–576. <https://doi.org/10.1212/WNL.0000000000002350>
  56. Scherfler C, Gobel G, Muller C, Nocker M, Wenning GK, Schocke M et al (2016) Diagnostic potential of automated subcortical volume segmentation in atypical parkinsonism. *Neurology* 86:1242–1249. <https://doi.org/10.1212/WNL.0000000000002518>
  57. Schrag A, Ben-Shlomo Y, Quinn N (2002) How valid is the clinical diagnosis of Parkinson's disease in the community? *J Neurol Neurosurg Psychiatry* 73:529–534
  58. Sekiya H, Kowa H, Koga H, Takata M, Satake W, Futamura N et al (2019) Wide distribution of  $\alpha$ -synuclein oligomers in multiple system atrophy brain detected by proximity ligation. *Acta Neuropathol* 137:455–466. <https://doi.org/10.1007/s00401-019-01961-w>
  59. Shahnawaz M, Mukherjee A, Pritzkow S, Mendez N, Rabadia P, Liu X et al (2020) Discriminating  $\alpha$ -synuclein strains in Parkinson's disease and multiple system atrophy. *Nature* 578:273–277. <https://doi.org/10.1038/s41586-020-1984-7>
  60. Shi M, Kovac A, Korff A, Cook TJ, Ginghina C, Bullock KM et al (2016) CNS tau efflux via exosomes is likely increased in Parkinson's disease but not in Alzheimer's disease. *Alzheimers Dement* 12:1125–1131. <https://doi.org/10.1016/j.jalz.2016.04.003>
  61. Shi M, Liu C, Cook TJ, Bullock KM, Zhao Y, Ginghina C et al (2014) Plasma exosomal  $\alpha$ -synuclein is likely CNS-derived and increased in Parkinson's disease. *Acta Neuropathol* 128:639–650. <https://doi.org/10.1007/s00401-014-1314-y>
  62. Skinner TR, Scott IA, Martin JH (2016) Diagnostic errors in older patients: a systematic review of incidence and potential causes in seven prevalent diseases. *Int J Gen Med* 9:137–146. <https://doi.org/10.2147/IJGM.S96741>
  63. Thery C, Ostrowski M, Segura E (2009) Membrane vesicles as conveyors of immune responses. *Nat Rev Immunol* 9:581–593. <https://doi.org/10.1038/nri2567>
  64. Tibshirani R (1996) Regression shrinkage and selection via the Lasso. *J Roy Stat Soc B Met* 58:267–288. <https://doi.org/10.1111/j.2517-6161.1996.tb02080.x>
  65. Tong J, Wong H, Guttman M, Ang LC, Forno LS, Shimadzu M et al (2010) Brain  $\alpha$ -synuclein accumulation in multiple system atrophy, Parkinson's disease and progressive supranuclear palsy: a comparative investigation. *Brain* 133:172–188. <https://doi.org/10.1093/brain/awp282>
  66. Trapp BD, Bernier L, Andrews SB, Colman DR (1988) Cellular and subcellular distribution of 2',3'-cyclic nucleotide 3'-phosphodiesterase and its mRNA in the rat central nervous system. *J Neurochem* 51:859–868. <https://doi.org/10.1111/j.1471-4159.1988.tb01822.x>
  67. Wakabayashi K, Hayashi S, Kakita A, Yamada M, Toyoshima Y, Yoshimoto M et al (1998) Accumulation of  $\alpha$ -synuclein/NACP is a cytopathological feature common to Lewy body disease and multiple system atrophy. *Acta Neuropathol* 96:445–452
  68. Walsh RR, Krismer F, Wenning GK, Low PA, Halliday GM, Koroshetz WJ et al (2017) Recommendations of the global multiple system atrophy research roadmap meeting. *Neurology* 90(2):74–82
  69. Wang Y, Shi M, Chung KA, Zabetian CP, Leverenz JB, Berg D et al (2012) Phosphorylated  $\alpha$ -synuclein in Parkinson's disease. *Sci Transl Med* 4:121ra120. <https://doi.org/10.1126/scitranslmed.3002566>
  70. Yu Z, Shi M, Stewart T, Fernagut PO, Huang Y, Tian C et al (2020) Reduced oligodendrocyte exosome secretion in multiple system atrophy involves SNARE dysfunction. *Brain*. <https://doi.org/10.1093/brain/awaa110>

**Publisher's Note** Springer Nature remains neutral with regard to jurisdictional claims in published maps and institutional affiliations.

## Authors and Affiliations

Suman Dutta<sup>1</sup> · Simon Hornung<sup>1,14</sup> · Adira Kruayatidee<sup>1</sup> · Katherine N. Maina<sup>1</sup> · Irish del Rosario<sup>2</sup> · Kimberly C. Paul<sup>2</sup> · Darice Y. Wong<sup>1</sup> · Aline Duarte Folle<sup>2</sup> · Daniela Markovic<sup>3</sup> · Jose-Alberto Palma<sup>4</sup> · Geidy E. Serrano<sup>5</sup> · Charles H. Adler<sup>6</sup> · Susan L. Perlman<sup>1</sup> · Wayne W. Poon<sup>7</sup> · Un Jung Kang<sup>4</sup> · Roy N. Alcalay<sup>8</sup> · Miriam Sklerov<sup>9</sup> · Karen H. Gyls<sup>10,12</sup> · Horacio Kaufmann<sup>4</sup> · Brent L. Fogel<sup>1,11,12</sup> · Jeff M. Bronstein<sup>1,12</sup> · Beate Ritz<sup>2,12</sup> · Gal Bitan<sup>1,12,13</sup> 

<sup>1</sup> Department of Neurology, David Geffen School of Medicine, University of California, Los Angeles, CA 90095, USA

<sup>2</sup> Department of Epidemiology, Fielding School of Public Health, University of California, Los Angeles, CA 90095, USA

- <sup>3</sup> Department of Medicine, Division of General Internal Medicine and Health Services Research, David Geffen School of Medicine, University of California, Los Angeles, CA 90095, USA
- <sup>4</sup> Department of Neurology, Dysautonomia Center, The Marlene and Paolo Fresco Institute for Parkinson's and Movement Disorders, New York University School of Medicine, New York, NY 10016, USA
- <sup>5</sup> Banner Sun Health Research Institute, Sun City, AZ 85351, USA
- <sup>6</sup> Mayo Clinic College of Medicine, Mayo Clinic Arizona, Scottsdale, AZ 85259, USA
- <sup>7</sup> Institute for Memory Impairments and Neurological Disorders, University of California, Irvine, CA 92697, USA
- <sup>8</sup> Department of Neurology, Taub Institute for Research on Alzheimer's Disease and the Aging Brain, Columbia University, New York, NY 10032, USA
- <sup>9</sup> Department of Neurology, University of North Carolina School of Medicine, Chapel Hill, NC 27599, USA
- <sup>10</sup> School of Nursing, University of California, Los Angeles, CA 90095, USA
- <sup>11</sup> Clinical Neurogenomics Research Center, David Geffen School of Medicine, University of California, Los Angeles, CA 90095, USA
- <sup>12</sup> Brain Research Institute, University of California, Los Angeles, CA 90095, USA
- <sup>13</sup> Molecular Biology Institute, University of California, Los Angeles, CA 90095, USA
- <sup>14</sup> Present Address: Division of Peptide Biochemistry, Technical University of Munich, 85354 Freising, Germany

## Supplementary Information

### **$\alpha$ -Synuclein in blood exosomes immunoprecipitated using neuronal and oligodendroglial markers distinguishes Parkinson's disease from multiple system atrophy**

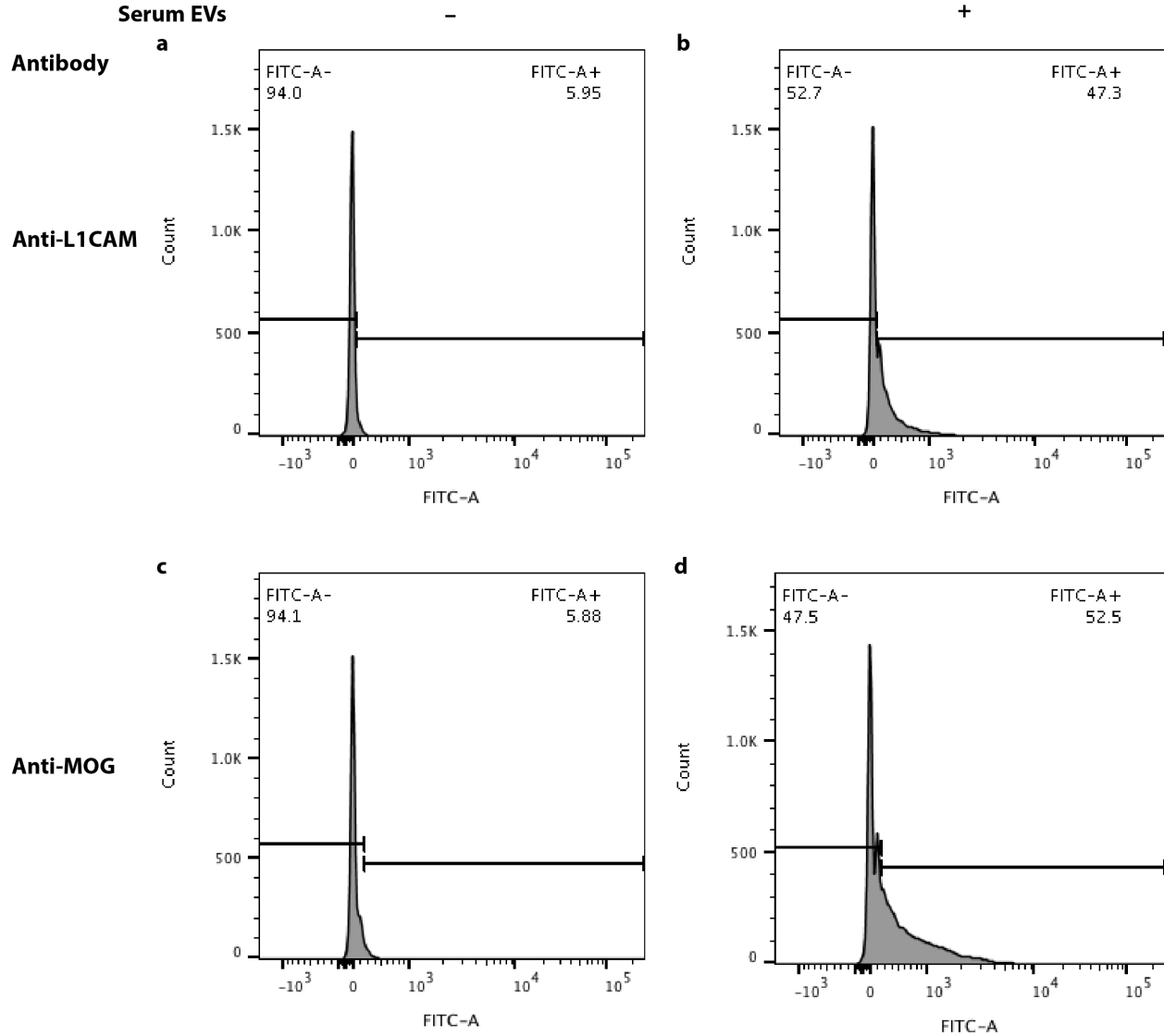
Suman Dutta<sup>1</sup>, Simon Hornung<sup>1†</sup>, Adira Kruayatidee<sup>1</sup>, Katherine N. Maina<sup>1</sup>, Irish del Rosario<sup>2</sup>, Kimberly C. Paul<sup>2</sup>, Darice Wong<sup>1</sup>, Aline Duarte Folle<sup>2</sup>, Daniela Markovic<sup>3</sup>, Jose-Alberto Palma<sup>4</sup>, Geidy E. Serrano<sup>5</sup>, Charles H. Adler<sup>6</sup>, Susan L. Perlman<sup>1</sup>, Wayne W. Poon<sup>7</sup>, Un Jung Kang<sup>4</sup>, Roy N. Alcalay<sup>8</sup>, Miriam Sklerov<sup>9</sup>, Karen H. Gyls<sup>10,12</sup>, Horacio Kaufmann<sup>4</sup>, Brent L. Fogel<sup>1,11,12</sup>, Jeff M. Bronstein<sup>1,12</sup>, Beate Ritz<sup>2,12</sup>, Gal Bitan,<sup>1,12,13\*</sup>

### **Supplementary Results**

Exosome isolation, enrichment, and validation. The first step in our process was the isolation from serum or plasma a mixture of extracellular vesicles (EVs) containing mainly exosomes by using System Biosciences' ExoQuick kit, according to methods described previously by Goetzl, Kapogiannis, and others [7, 11, 21]. We and others have shown previously that this step yields a mixture of EVs, including exosomes, ectosomes, and some cell debris [4, 9, 22], in which we found that exosomes comprised 90–95% of the particle population using tunable resistive pulse sensing (TRPS), which showed a mean diameter of  $143 \pm 47$  nm, and  $d_{90} = 189$  (i.e., 90% of the vesicles had a diameter below 189 nm) [22]. Western blot analysis probing for the exosomal protein markers Alix, CD9, and CD81 confirmed that these markers were highly enriched in the exosomes compared to their concentration in crude serum [22].

Next, we immunoprecipitated exosomes using magnetic beads conjugated to antibodies against the neuronal marker L1CAM, as described previously [10, 17, 21], or the oligodendrocyte marker MOG. We chose MOG for isolation of oligodendroglial exosomes because it is a membrane-bound protein, highly specific to mature oligodendrocytes, and monoclonal antibodies recognizing the extracellular domain of the protein, which is required for successful immunoprecipitation, are commercially available. To confirm exosome capture, anti-L1CAM- or anti-MOG antibody-conjugated beads were incubated either with EVs derived from commercial, pooled human serum using the ExoQuick kit and resuspended in PBS containing 1% BSA and PPI, or with only PBS + 1% BSA and PPI. The beads then were washed in PBS + 0.1% BSA and incubated with a fluorescein isothiocyanate (FITC)-tagged anti-CD9 antibody followed by a flow-cytometry analysis. Only beads that captured exosomes would be expected to be labeled by the FITC-tagged antibody. The data showed an 8–9-fold increase in the number of FITC-positive beads incubated with human serum derived EVs (Supplementary fig. 1b, d) compared to non-specific binding of the antibody to the negative-control beads incubated with buffer only (Supplementary fig. 1a, c), demonstrating successful capture of exosomes on these beads.

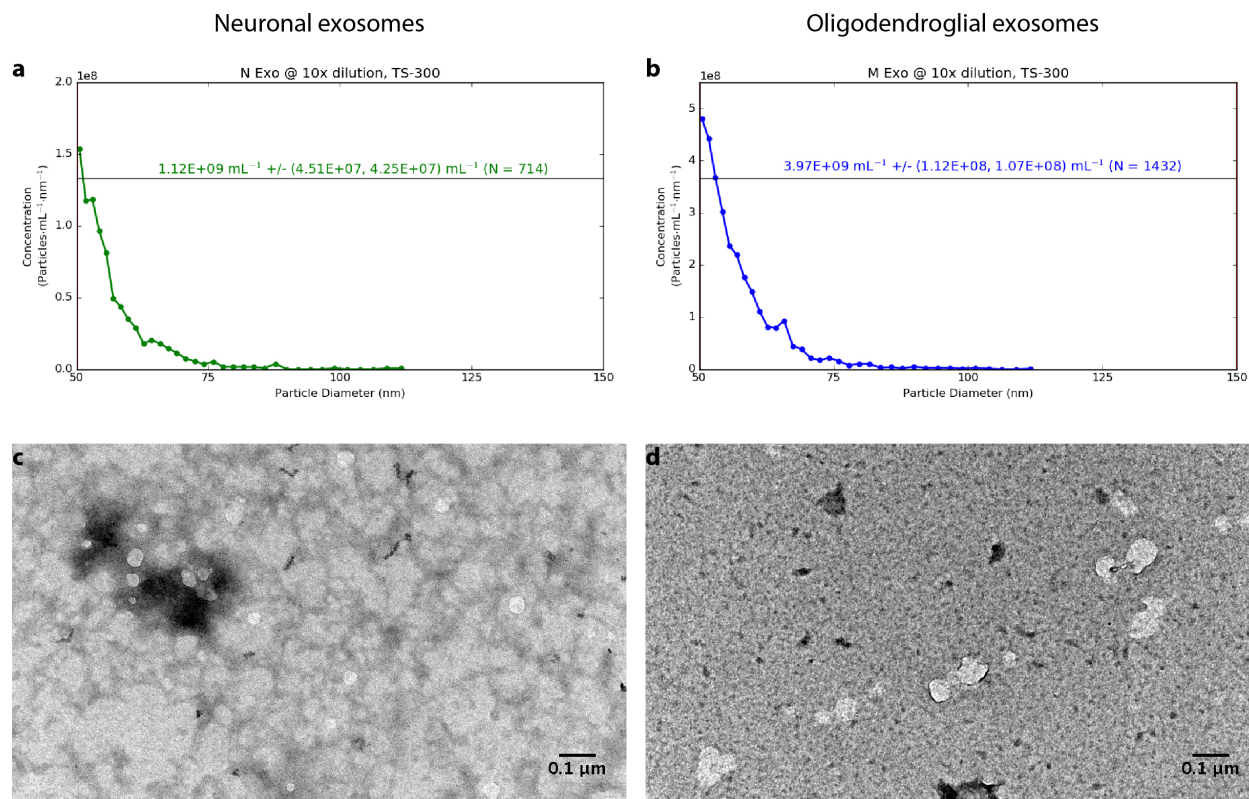
We assessed the size distribution of the captured exosomes using Microfluidic Resistive Pulse Sensing (MRPS) and verified that their morphology remained intact by transmission electron microscopy (TEM) analysis. The MRPS analysis showed that the diameter distribution of the captured exosomes was 50–150 (Supplementary fig. 2a, b), consistent with the expected range of exosomes. The morphological analysis confirmed that the eluted exosomes were intact and had the expected morphology and appearance (Supplementary fig. 2c, d).



**Supplementary Fig. 1. Exosomes are captured by magnetic beads conjugated to anti-L1CAM or anti-MOG antibodies.** Anti-L1CAM- (a, b) or anti-MOG- (c, d) conjugated magnetic beads were incubated either with PBS containing 1% BSA (a, c) or with the same buffer containing EVs isolated from human serum (b, d). The beads then were washed and incubated with a FITC-conjugated anti-CD9 antibody. CD9-positive beads (i.e., those that bound exosomes) were quantified by flow-cytometry.

L1CAM is a heterogeneous protein due to alternative splicing, glycosylation, truncation, and other post-translational modifications [1, 8, 16], which recently has prompted Norman et al. to raise a concern regarding the ability of antibodies against this protein to capture *bona fide* CNS-originating exosomes [13]. To address this concern, we fractionated human pooled serum or pooled plasma using the same size-exclusion column used by Norman et al., which is designed for separation of exosomes and other extracellular vesicles from serum/plasma proteins. We then assessed the fractions for the presence of L1CAM using a commercial ELISA kit. The analysis showed that although most of the L1CAM signal was found in the fractions containing free proteins, as reported by Norman et al., all the fractions containing exosomes from the serum or plasma were L1CAM-positive (Supplementary fig. 3). No signal was detected in 50  $\mu$ L PBS or 25  $\mu$ L RIPA buffer (data not shown), excluding matrix effects.

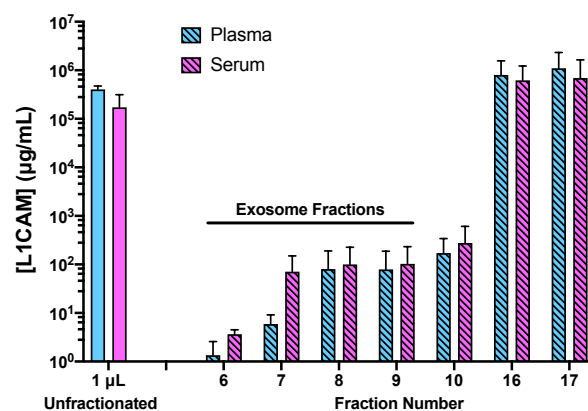




**Supplementary Fig. 2. Characterization of immunoprecipitated exosome size distribution and morphology.** Exosomes were eluted from magnetic beads conjugated to anti-L1CAM (a, c) or anti-MOG (b, d) antibodies. a, b) Particle size-distribution analysis by MRPS. c, d) Transmission electron micrographs of the captured exosomes after release from the beads. The scale bar represents 0.1 μm. The size variation reflects the range of exosome diameters.

The large difference in concentration might raise the concern that free L1CAM in the serum or plasma could saturate the antibody-conjugated beads, precluding binding of the minute quantities of exosomes displaying L1CAM on their surface. This is a valid concern for a one-step process attempting to isolate the exosomes directly from the biofluid, as was described by some groups [10, 18], but not in a two-step process in which EVs are separated first from the biofluid, removing free L1CAM, as was done here, and only then are incubated with the antibody-conjugated beads. Thus, our data support the notion that L1CAM can be used to enrich CNS-originating exosomes by immunoprecipitation.

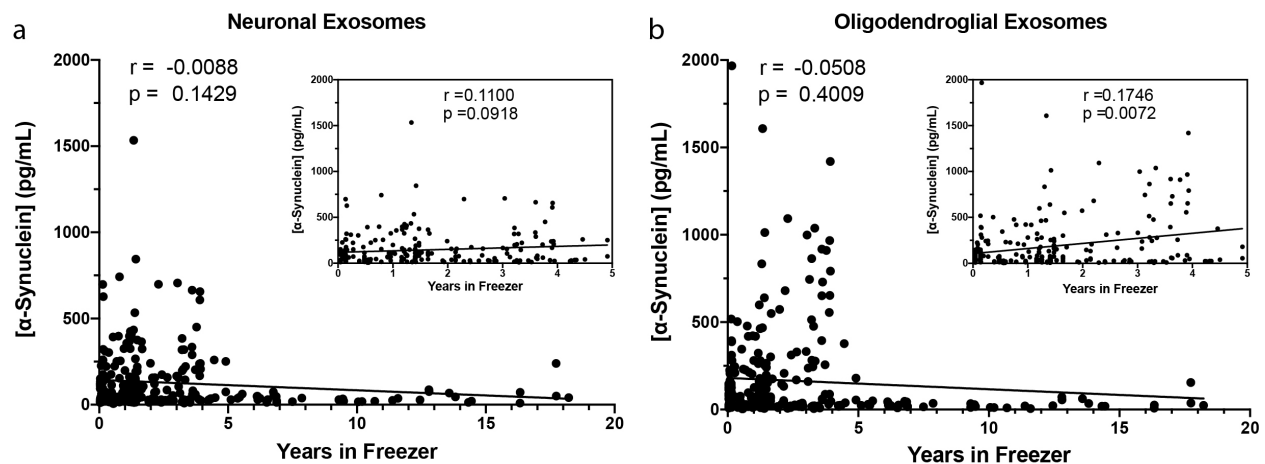
Norman et al. [13] also reported that magnetic beads conjugated to the anti-



**Supplementary Fig. 3. Analysis of L1CAM in human serum and plasma.** Serum or plasma were fractionated using a qEVoriginal size-exclusion chromatography column (Izon Sciences). Fractions were collected and analyzed for the presence of L1CAM using ELISA. Exosomes are eluted in fractions 6–9. The graph represents two independent experiments.

L1CAM antibody UJ127 [6] displayed relatively high binding of  $\alpha$ -syn, suggesting cross-reactivity of this antibody with  $\alpha$ -syn. We used only the anti-L1CAM antibody 5G3 [12] and have tested the level of  $\alpha$ -syn binding to beads conjugated to this antibody, the anti-MOG antibody D-2 used for immunoprecipitation of oligodendroglial exosomes, or a control mouse IgG. In all cases, using electrochemiluminescence ELISA (ECLIA), we found similar amounts of non-specifically bound  $\alpha$ -syn to the antibody-conjugated beads, which were 42–60-times lower than those reported by Norman et al.

**Characterization of  $\alpha$ -syn measurement reproducibility.** After immunoprecipitating the exosomes, we lysed them and used ECLIA (Meso Scale Discovery) to measure  $\alpha$ -syn concentration. The dynamic range reported by the company is 8.00–6,800 pg/mL and the lower limit of detection (LLoD) is 0.9 pg/mL. In our hands, using the  $\alpha$ -syn standard provided by the manufacturer, the average LLoD was 2.6 pg/mL and the lower limit of quantitation (LLoQ) was 4.0 pg/mL. Because the variability involved in the exosome isolation process is substantially higher than in simple measurements of the recombinant  $\alpha$ -syn standard, we determined the intra- and inter-assay coefficient of variation (CV) using putative neuronal exosomes isolated from commercial, human pooled serum in three independent experiments, each with three technical replicates. Our experiments yielded, intra-experiment CV = 7.1%, and inter-experiment CV = 8.8%, demonstrating a high reproducibility of the process and the assay.



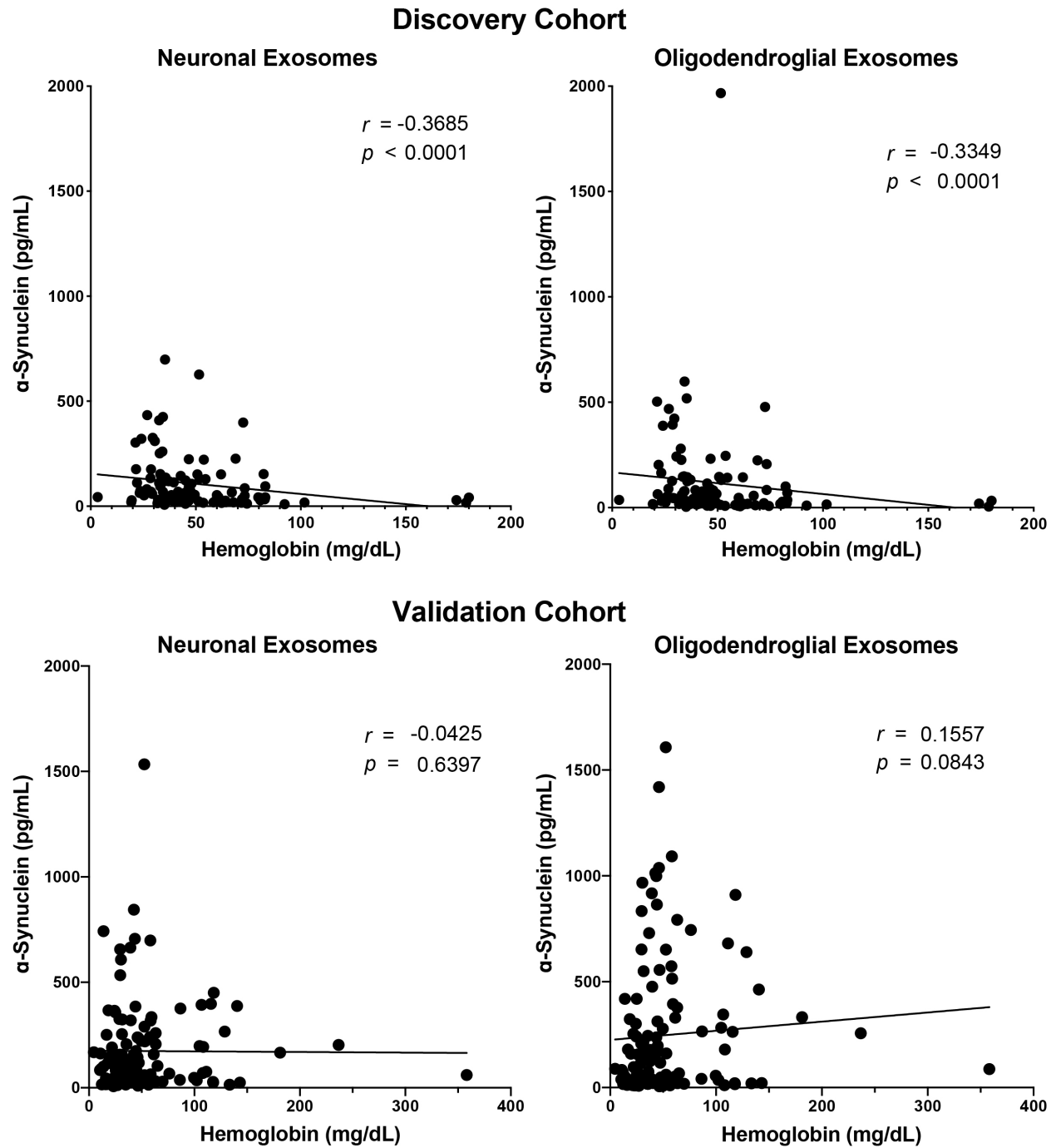
**Supplementary Fig. 4. Exosomal  $\alpha$ -syn stability.** Stability was evaluated by correlating the  $\alpha$ -syn concentration in putative neuronal (a) or oligodendroglial (b) exosomes with the time the samples were stored at  $-80^{\circ}\text{C}$ . The insets in each panel show the correlation for the subset of samples stored for  $\leq 5$  years.

**$\alpha$ -Syn signal in CNS-originating exosomes decreases sharply after 5 years.** Our initial discovery cohort comprised 51 control, 50 PD, and 30 MSA samples, whereas the validation cohort consisted of 50 samples in each group. The samples for the validation cohort were obtained separately, after analysis of the discovery cohort was completed. Between the time of collection and the time of measurement, the samples were stored at  $-80^{\circ}\text{C}$  for a wide range of periods, between 15 and 6,650 days ( $> 18$  years). Therefore, we asked whether storage for a long period might compromise the stability of  $\alpha$ -syn in the samples. Indeed, a Spearman-correlation analysis showed that  $\alpha$ -syn concentration declined slightly over time. The decline was similar in the putative neuronal

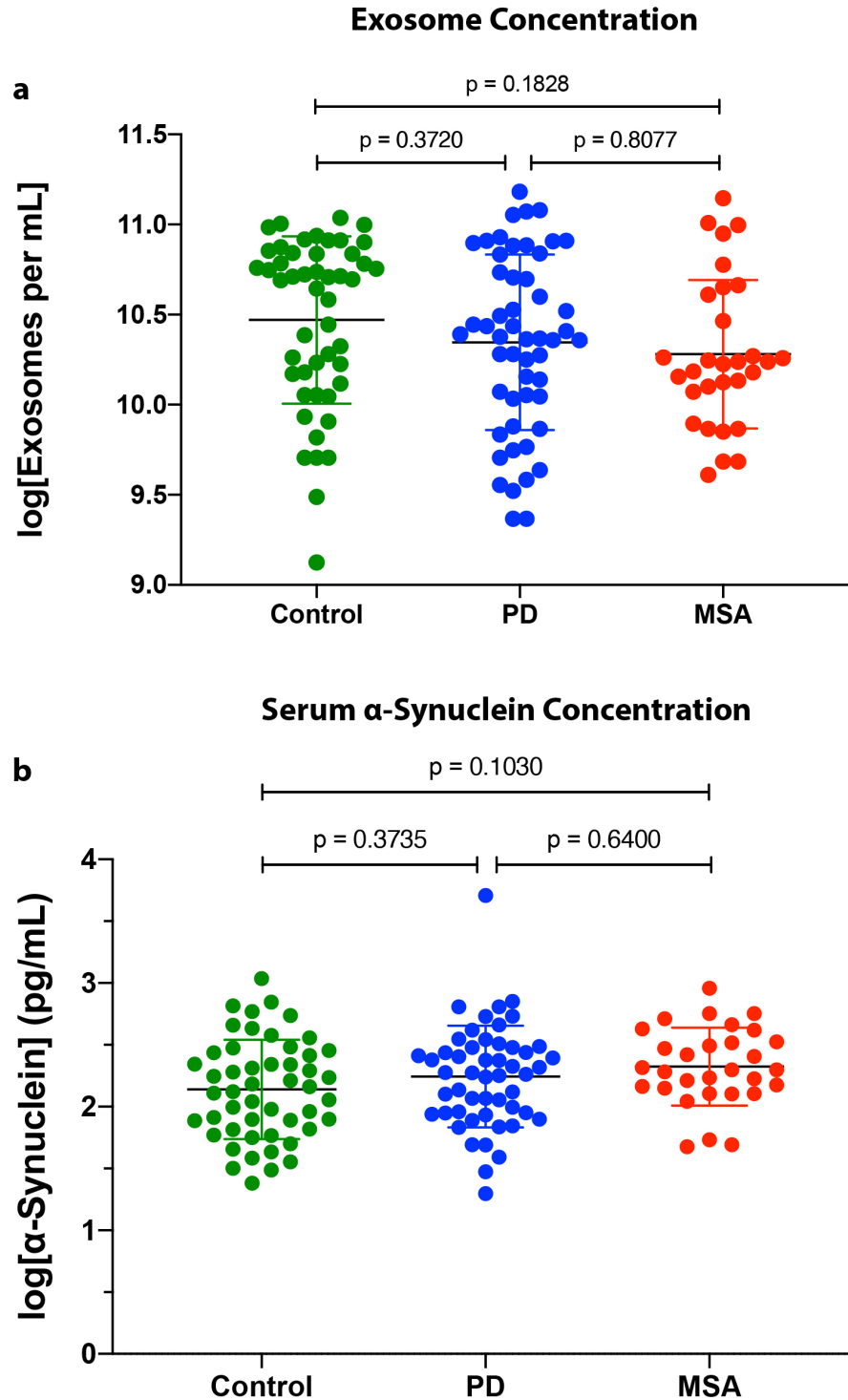
(Supplementary fig. 4a) and oligodendroglial (Supplementary fig. 4b) exosomes. However, rather than a linear decline, the data suggested that the samples were stable for ~5 years, after which the average signal declined sharply. Thus, the same correlation analysis in samples stored for  $\leq 5$  years (insets in Supplementary figs. 5a, b) no longer showed the decline in  $\alpha$ -syn concentration. In fact, in the putative oligodendroglial exosomes, the signal seemed to increase with time, though this likely represents a statistical anomaly rather than a real physical phenomenon. In view of these results, we excluded all the samples stored  $> 5$  years, a total of 45 samples in the two cohorts, from further data analysis and replaced them with 45 new, different samples from the same collaborators, stored for  $< 5$  years, which were randomized between the discovery and validation cohorts to restore approximately the same sample numbers.

$\alpha$ -Syn normalization and origin. Although some reports of similar measurements used normalization of exosome biomarker concentrations to the exosomal marker CD81, we chose to normalize the  $\alpha$ -syn concentration to total protein (measured using a BCA assay) in the exosome preparation from each cell type because CD81 (and other tetraspanin) concentrations may vary among exosomes under different conditions [19, 20] and how they are impacted by neurodegenerative diseases currently is not known. We used a CD81 ELISA only to compare the number of exosomes among samples before enrichment of CNS exosomes.

Because erythrocytes are rich in  $\alpha$ -syn [2], their hemolysis could release  $\alpha$ -syn into the serum/plasma. As  $\alpha$ -syn is known to have a high affinity for lipid membranes [5, 14, 15], it could bind to exosomes and generate false results in our assay. To minimize hemolysis, all the samples were processed within 30 min following blood draw. Nonetheless, to test whether erythrocyte  $\alpha$ -syn was present in meaningful amounts, we measured hemoglobin in all the samples and tested whether a linear correlation could be found between the hemoglobin concentration in the serum/plasma and the  $\alpha$ -syn concentration in the putative CNS-originating exosomes (Supplementary fig. 5). If erythrocyte  $\alpha$ -syn contamination contributed meaningfully to the signal measured in the exosomes, the signal would be expected to increase in correlation with increasing serum/plasma hemoglobin concentration. The analysis showed that such a correlation was not found between serum hemoglobin and putative CNS-exosomal  $\alpha$ -syn, suggesting that the measured  $\alpha$ -syn in the exosomes plausibly originated in the CNS and was not contaminated meaningfully by erythrocytic  $\alpha$ -syn.



**Supplementary Fig. 5. Spearman-correlation analysis between serum/plasma hemoglobin and putative CNS-exosomal  $\alpha$ -syn.** The lack of correlation suggests that the exosomal  $\alpha$ -syn did not originate in erythrocytes.



**Supplementary Fig. 6. Measurement of exosome concentration and serum  $\alpha$ -syn before exosome immunoprecipitation in the discovery cohort.** a) Exosome concentration was estimated using a CD81 ELISA (Systems Biosciences) and the reading was converted to exosome concentration according to the manufacturer's instructions and log-transformed. b)  $\alpha$ -Syn concentration was measured in 0.5  $\mu$ L serum using ECLIA and log-transformed. P-values were calculated by a one-way ANOVA with post hoc Tukey test.



**Supplementary Table 1. Comparison between the biomarkers across providing clinics in the discovery and validation cohorts.**

| Cohort     | Diagnosis  | Source   | N  | Putative Neuronal $\alpha$ -syn (pg/mL) | P-value                  | Putative Oligodendroglial $\alpha$ -syn (pg/mL) | P-value                  | Oligo: Neuro ratio | P-value                  |
|------------|--|----------|----|---|--------------------------|---|--------------------------|--------------------|--------------------------|
| Discovery  | Control  | UCLA     | 50 | 57.2 $\pm$ 55.6                         | n/a                      | 52.7 $\pm$ 73.0                                 | n/a                      | 0.837 $\pm$ 0.413  | n/a                      |
|            |  | NYU      | 1  | 43.8                                    |                          | 36.3  |                          | 0.829              |                          |
|            | PD   | UCLA     | 47 | 89.5 $\pm$ 106.0                        | n/a                      | 62.9 $\pm$ 79.7                                 | n/a                      | 0.702 $\pm$ 0.259  | n/a                      |
|            |  | NYU      | 4  | 316.1 $\pm$ 146.5                       |                          | 298.2 $\pm$ 117.5                               |                          | 1.091 $\pm$ 0.514  |                          |
|            | MSA  | UCLA     | 21 | 149.2 $\pm$ 79.9                        | 0.006 <sup>1</sup>       | 197.4 $\pm$ 111.9                               | 0.032 <sup>1</sup>       | 1.390 $\pm$ 0.545  | 0.879 <sup>1</sup>       |
|            |  | NYU      | 9  | 288.2 $\pm$ 176.6                       |                          | 491.0 $\pm$ 583.0                               |                          | 1.426 $\pm$ 0.679  |                          |
| Validation | Control  | UCLA     | 24 | 167.0 $\pm$ 174.6                       | 0.0003 <sup>1</sup>      | 100.8 $\pm$ 120.2                               | 0.0024 <sup>1</sup>      | 0.681 $\pm$ 0.370  | 0.269 <sup>1</sup>       |
|            |  | NYU      | 0  | -                                       |                          | -   |                          | -                  |                          |
|            |  | Columbia | 26 | 32.8 $\pm$ 29.1                         |                          | 24.5 $\pm$ 16.3                                 |                          | 0.786 $\pm$ 0.291  |                          |
|            | PD   | UCLA     | 50 | 94.3 $\pm$ 90.7                         | n/a                      | 76.4 $\pm$ 75.9                                 | n/a                      | 0.857 $\pm$ 0.391  | n/a                      |
|            |  | NYU      | 3  | 376.2 $\pm$ 405.7                       |                          | 427.4 $\pm$ 507.5                               |                          | 1.032 $\pm$ 0.147  |                          |
|            |  | Columbia | 0  | -                                       |                          | -   |                          | -                  |                          |
|            | MSA  | UCLA     | 9  | 377.1 $\pm$ 460.5                       | U-N – 0.449 <sup>2</sup> | 421.8 $\pm$ 481.6                               | U-N – 0.826 <sup>2</sup> | 1.446 $\pm$ 0.895  | U-N – 0.968 <sup>2</sup> |
|            |  | NYU      | 7  | 222.7 $\pm$ 103.9                       | U-C – 0.510 <sup>2</sup> | 316.0 $\pm$ 254.5                               | U-C – 0.584 <sup>2</sup> | 1.726 $\pm$ 1.770  | U-C – 0.313 <sup>2</sup> |
|            |  | Columbia | 34 | 271.9 $\pm$ 192                         | N-C – 0.885 <sup>2</sup> | 554.4 $\pm$ 335.0                               | N-C – 0.250 <sup>2</sup> | 2.699 $\pm$ 2.561  | N-C – 0.559 <sup>2</sup> |
|            | <sup>1</sup> P-value calculated by Student's t-test. <sup>2</sup> P-value calculated by one-way ANOVA, U-N – UCLA vs NYU, U-C – UCLA vs Columbia, N-C – NYU vs Columbia. |          |    |   |                          |   |                          |                    |                          |

Post-mortem samples cannot be used for measurement of  $\alpha$ -syn in putative CNS-originating exosomes. A potential source of pathologically validated serum samples of patients with synucleinopathies and healthy controls are samples collected post-mortem with a short post-mortem interval (PMI) [3]. A concern in using post-mortem samples in our assay is hemolysis of erythrocytes, which are rich in  $\alpha$ -syn [2]. Such hemolysis could release  $\alpha$ -syn into the blood, leading to binding of the released  $\alpha$ -syn to lipid membranes, including those of exosomes, thus preventing meaningful analysis of CNS-originating  $\alpha$ -syn in exosomes. However, whether this is only a theoretical problem or a practical one is not known. As explained above, this question can be addressed by testing whether the concentration of  $\alpha$ -syn in the exosomes correlates with the concentration of hemoglobin in the serum. If a significant correlation is found, a substantial fraction of the  $\alpha$ -syn signal likely originates in erythrocytes and the samples cannot be used.

To test whether post-mortem samples could be used for this purpose, we obtained serum samples from the Banner Sun Health Research Institute, Scottsdale, AZ, which were collected within  $\leq 6$  h from 49 patients with PD and 12 patients with MSA (Supplementary Table 2) whose disease was validated pathologically. We measured hemoglobin in these samples as described above, and then isolated putative neuronal and oligodendroglial exosomes and tested whether the  $\alpha$ -syn and hemoglobin concentrations correlated. An initial warning sign was a significantly higher average exosome concentration, measured using a CD81 ELISA, in the post-mortem samples (PD –  $6.8 \times 10^{10} \pm 4.3 \times 10^{10}$ , MSA –  $5.4 \times 10^{10} \pm 1.7 \times 10^{10}$  exosomes/mL) compared to the pre-mortem samples (PD –  $3.3 \times 10^{10} \pm 3.4 \times 10^{10}$  exosomes/mL, MSA –  $3.1 \times 10^{10} \pm 3.4 \times 10^{10}$  exosomes/mL (Supplementary fig. 7a)), suggesting release of exosomes from cells undergoing necrosis. The data demonstrated that the exosomes were stable in the blood at least up to PMI = 6, yet the exosome

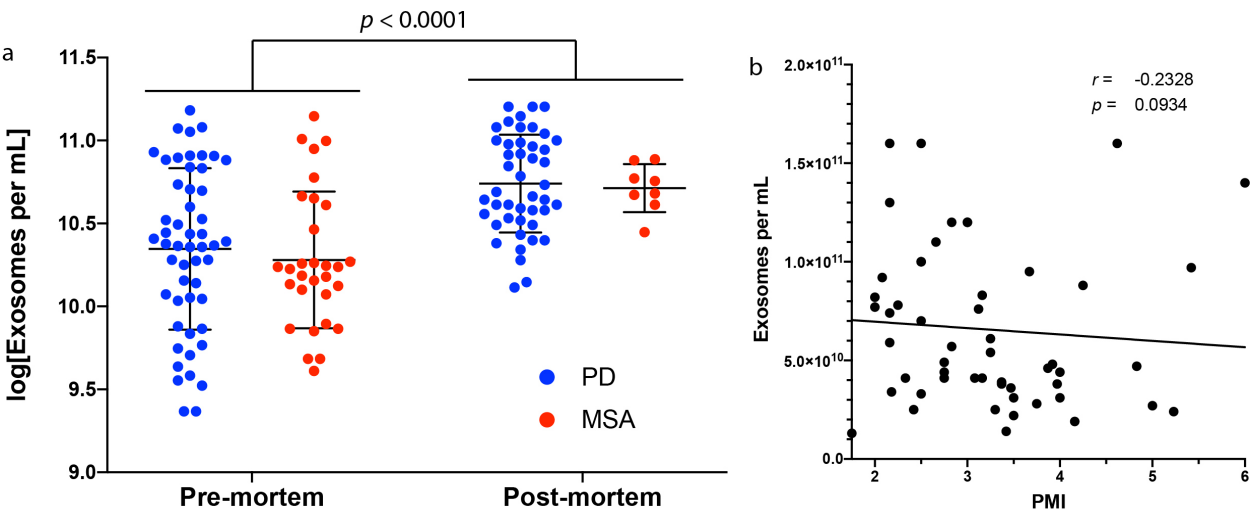
concentrations in these samples did not correlate meaningfully with PMI (Supplementary fig. 7b), suggesting that multiple mechanisms contributed to exosome release.

**Supplementary Table S2. Demographic details for postmortem samples used in the study**

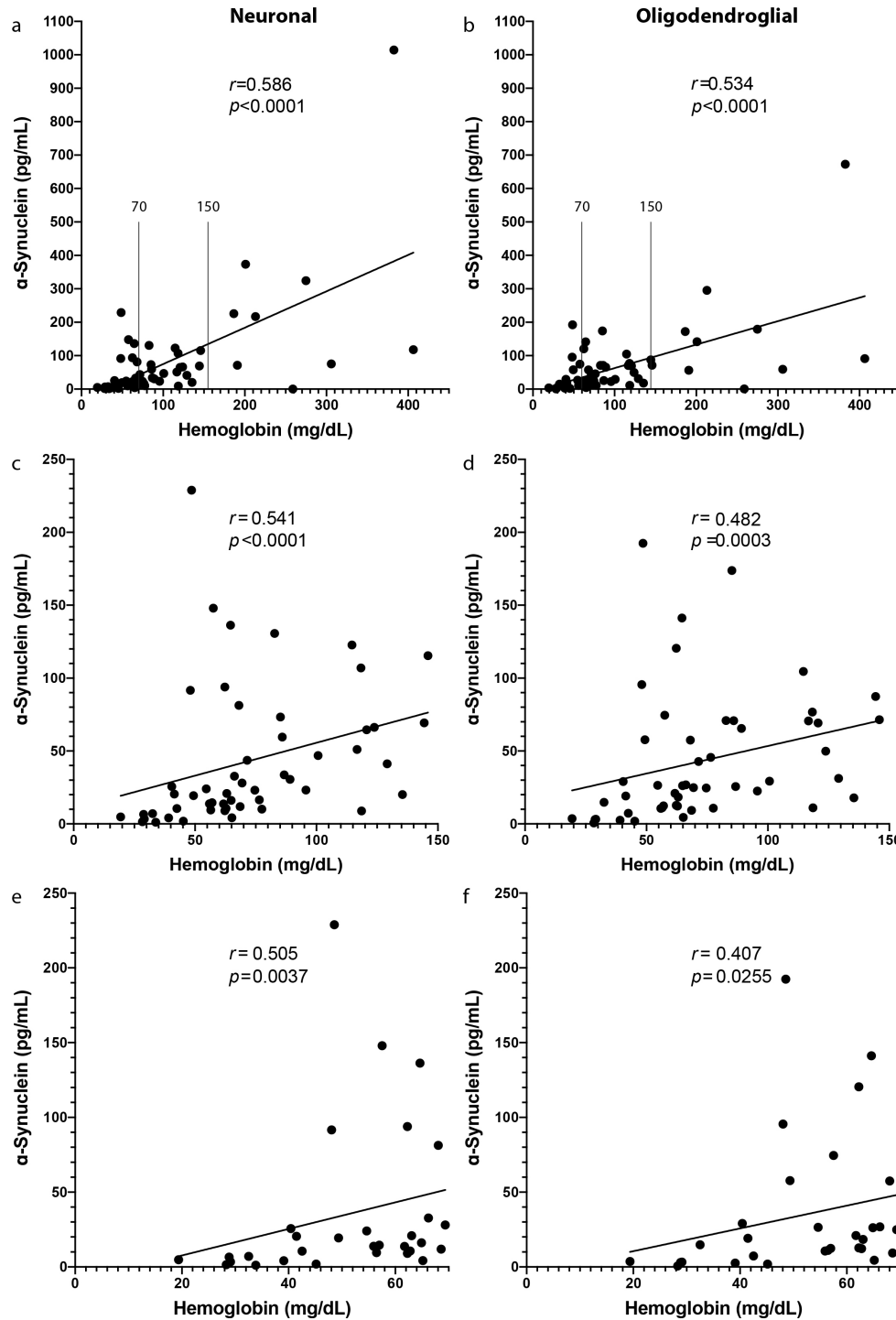
| Disease | Sample number | F:M   | Race  | Age at death (range) | PMI (range)         | UPDRS motor (range) | MMSE (range)      |
|---------|---------------|-------|---|----------------------|---------------------|---------------------|-------------------|
| PD      | 49            | 20:29 | White (49)                                  | 80.2 ± 5.8 (69–95)   | 3.2 ± 1.0 (1.8–6.0) | 36.3 ± 19.8 (6–80), | 22.3 ± 6.4 (0–29) |
| MSA     | 12            | 9:3   | African-American (1), Asian (1), White (10) | 70.5 ± 7.8 (60–84)   | 3.2 ± 0.9 (2.0–4.8) |                     |                   |

Spearman-correlation analysis showed that unlike in the samples collected from living patients (Supplementary fig. 5), strong positive correlations were found between both the putative neuronal and the putative oligodendroglial exosomal  $\alpha$ -syn and serum hemoglobin concentrations (Supplementary fig. 8a, b), suggesting that erythrocyte  $\alpha$ -syn was a major contributor to the signal in these samples. Neither the hemoglobin, nor the  $\alpha$ -syn concentrations in the putative neuronal or oligodendroglial exosomes correlated with PMI (data not shown), suggesting that multiple mechanisms were involved in hemolysis postmortem.

An attempt to set up a cutoff of hemoglobin concentration under which putative CNS-exosomal  $\alpha$ -syn concentrations might be used, as is often done in analysis of CSF biomarkers, did not eliminate the correlation even when the cutoff was set as low as 70 mg/dL hemoglobin, at which point ~40% of the samples were excluded (Supplementary figs. 8c–f).



**Supplementary Fig. 7. Exosome concentration in postmortem samples.** Exosome concentration was estimated using a CD81 ELISA. a) Exosome concentrations (log-transformed) were found to be higher in postmortem than in premortem samples ( $p < 0.0001$ , two-way ANOVA with post hoc Tukey test). b) Spearman-correlation analysis showed that exosome concentrations in the postmortem cohort did not correlate with PMI.

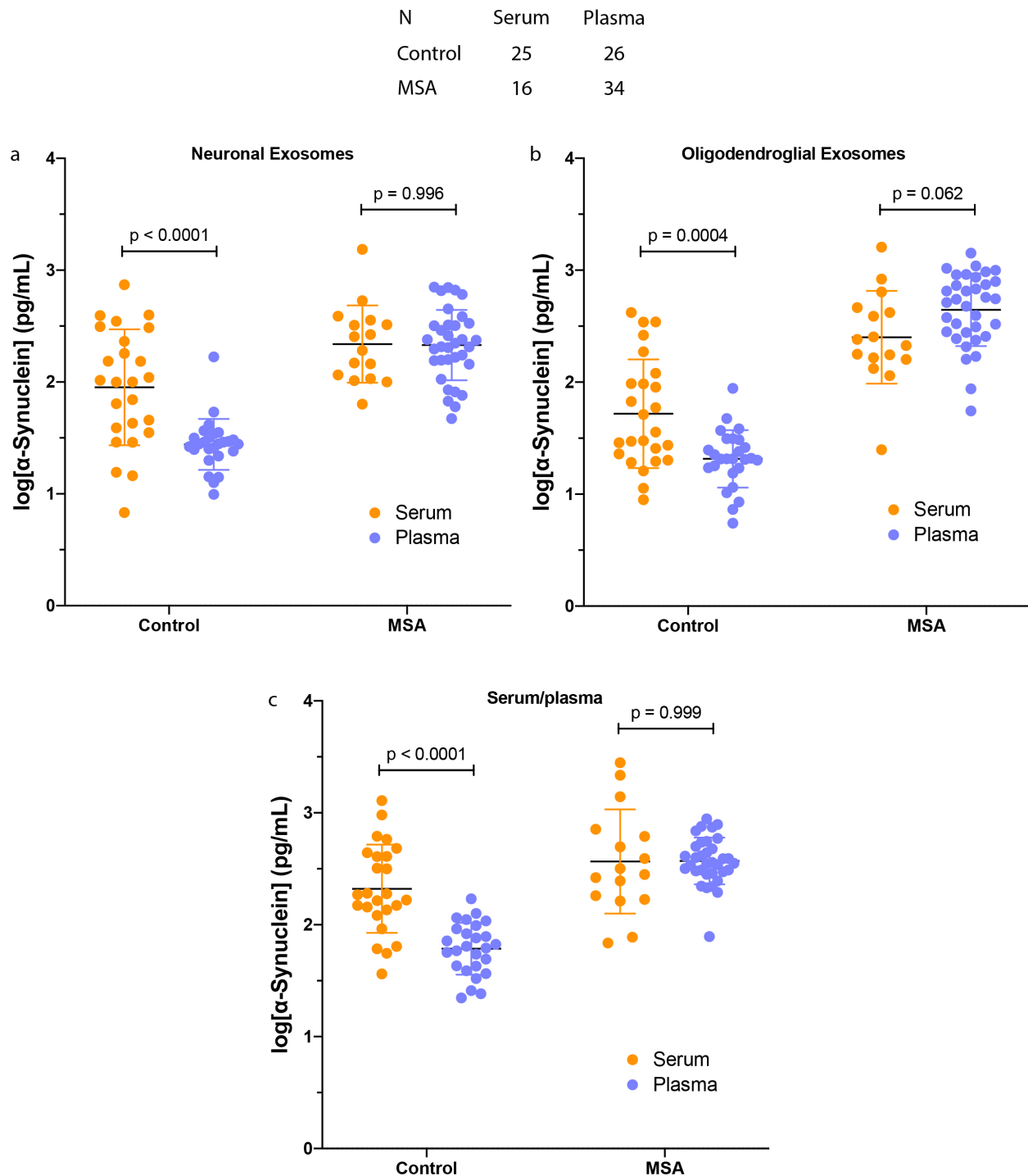


**Supplementary Fig. 8. Spearman correlation between serum hemoglobin and  $\alpha$ -syn measured in putative CNS-originating exosomes from postmortem samples.** a, b) Spearman correlation in putative neuronal (a) or oligodendroglial (b) exosomes shows a strong correlation between serum hemoglobin and exosomal  $\alpha$ -syn concentrations. Vertical lines indicate the cutoffs at 150 and 70 mg/dL hemoglobin. c, d) Spearman correlation in putative neuronal (c) or oligodendroglial (d) exosomes with a cutoff at 150 mg/dL hemoglobin. e, f) Spearman correlation in putative neuronal (e) or oligodendroglial (f) exosomes with a cutoff at 70 mg/dL hemoglobin.

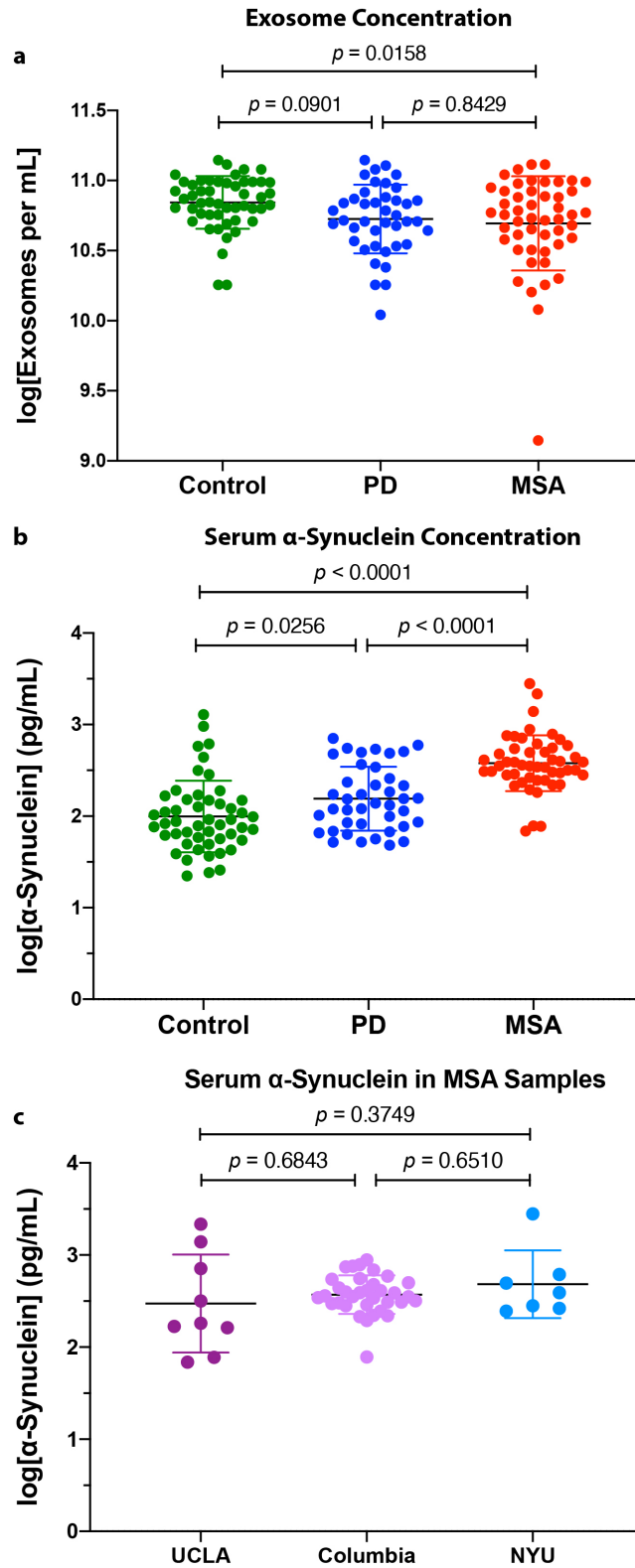
1 **Supplementary Table S3. Comparison of discovery and validation cohort composition.**

| Diagnosis       | Control     |            |         | PD         |             |         | MSA        |            |         |
|-----------------|-------------|------------|---------|------------|-------------|---------|------------|------------|---------|
| Cohort          | Discovery   | Validation | p-Value | Discovery  | Validation  | p-Value | Discovery  | Validation | p-Value |
| Male            | 22 (44.0%)  | 23 (45.1%) | 0.9116  | 32 (62.8%) | 33 (62.3%)  | 0.9596  | 13 (43.3%) | 26 (52.0%) | 0.4528  |
| Female          | 28 (56.0%)  | 28 (54.9%) | 0.9116  | 19 (37.3%) | 20 (37.7%)  | 0.9596  | 17 (56.7%) | 24 (48.0%) | 0.4528  |
| Age             | 63.2 ± 12.2 | 66.6 ± 8.9 | 0.1687  | 71.5 ± 9.5 | 72.0 ± 10.2 | 0.7572  | 62.7 ± 8.3 | 62.9 ± 7.9 | 0.8476  |
| Asian           | 1 (2.0%)    | 1 (2.0%)   | 0.7104  | 0 (0.0%)   | 1 (1.9%)    | 0.3950  | 7 (23.3%)  | 6 (12.0%)  | 0.6220  |
| Black           | 0 (0.0%)    | 0 (0.0%)   | 0.7104  | 1 (2.0%)   | 0 (0.0%)    | 0.3950  | 1 (3.3%)   | 4 (8.0%)   | 0.6220  |
| Hispanic        | 10 (20.0%)  | 10 (19.6%) | 0.7104  | 9 (17.1%)  | 11 (20.8%)  | 0.3950  | 1 (3.3%)   | 1 (2.0%)   | 0.6220  |
| Native American | 2 (4.0%)    | 1 (2.0%)   | 0.7104  | 1 (2.0%)   | 4 (7.6%)    | 0.3950  | 0 (0.0%)   | 0 (0.0%)   | 0.6220  |
| Not disclosed   | 1 (2.0%)    | 4 (7.8%)   | 0.7104  | 0 (0.0%)   | 1 (1.9%)    | 0.3950  | 1 (3.3%)   | 1 (2.0%)   | 0.6220  |
| White           | 36 (72.0)   | 35 (68.6%) | 0.7104  | 40 (78.4%) | 36 (67.9%)  | 0.3950  | 20 (66.7%) | 38 (76.0%) | 0.6220  |

2  
3 Adjustment of raw data in the validation cohort. Compared to serum samples, from which EVs  
4 can be precipitated directly, plasma samples require a preparatory step, digestion of fibrinogen  
5 with thrombin and clearance of the resulting fibrin by centrifugation. However, after initiating the  
6 analysis of this cohort, we discovered that a few plasma samples were mislabeled as serum and  
7 therefore this preparatory step was not included in the process. As a result, the measured exosomal  
8  $\alpha$ -syn concentrations in the mislabeled samples appeared to be an order of magnitude higher than  
9 those in serum samples. In order not to discard the results for these precious samples, we decided  
10 to exclude the thrombin digestion step in all the plasma samples. To allow subsequent analysis of  
11 the serum and plasma samples together, we measured  $\alpha$ -syn in neuronal exosomes isolated from  
12 commercial pooled serum or pooled plasma in three independent experiments, each done in three  
13 technical replicates and calculated the factor by which plasma samples gave a higher reading than  
14 serum samples to be  $11.3 \pm 1.8$ . We therefore divided the raw concentrations in all the plasma  
15 samples by 11.3 and after completing the analysis of this cohort, asked how the values of the serum  
16 samples compared to the adjusted plasma samples. In the putative neuronal exosomes, for the  
17 control group, the adjusted  $\alpha$ -syn concentrations in the plasma ( $33 \pm 29$  pg/mL, Supplementary  
18 fig.9a) were lower than in the serum ( $161 \pm 174$  pg/mL) whereas in the MSA group the  
19 concentrations were comparable (serum –  $310 \pm 352$  pg/mL, plasma –  $272 \pm 192$  pg/mL). In the  
20 putative oligodendroglial exosomes, for the control group, the adjusted plasma  $\alpha$ -syn  
21 concentrations ( $24 \pm 16$  pg/mL, Supplementary fig.9b) again were lower than in the serum ( $97 \pm$   
22  $119$  pg/mL), whereas in the MSA group, the plasma values ( $554 \pm 335$  pg/mL) were higher than  
23 in the serum ( $376 \pm 391$  pg/mL). Because the differences between the serum and plasma values  
24 were not consistently in a certain direction, we combined the values for the validation cohort yet  
25 kept these differences in mind when interpreting the data.



**Supplementary Fig. 9. Comparison between serum and plasma samples in the validation cohort.** Plasma samples were included in the control and MSA groups only. The numbers of serum and plasma samples in each group are shown at the top. a) Comparison of log-transformed  $\alpha$ -syn concentration in serum (direct measurement) and plasma (adjusted) in putative neuronal exosomes. b) The same measurement in putative oligodendroglial exosomes. c) The same measurement directly in the serum or plasma. P-values were calculated using a 2-way ANOVA with Sidak's multiple comparison test.



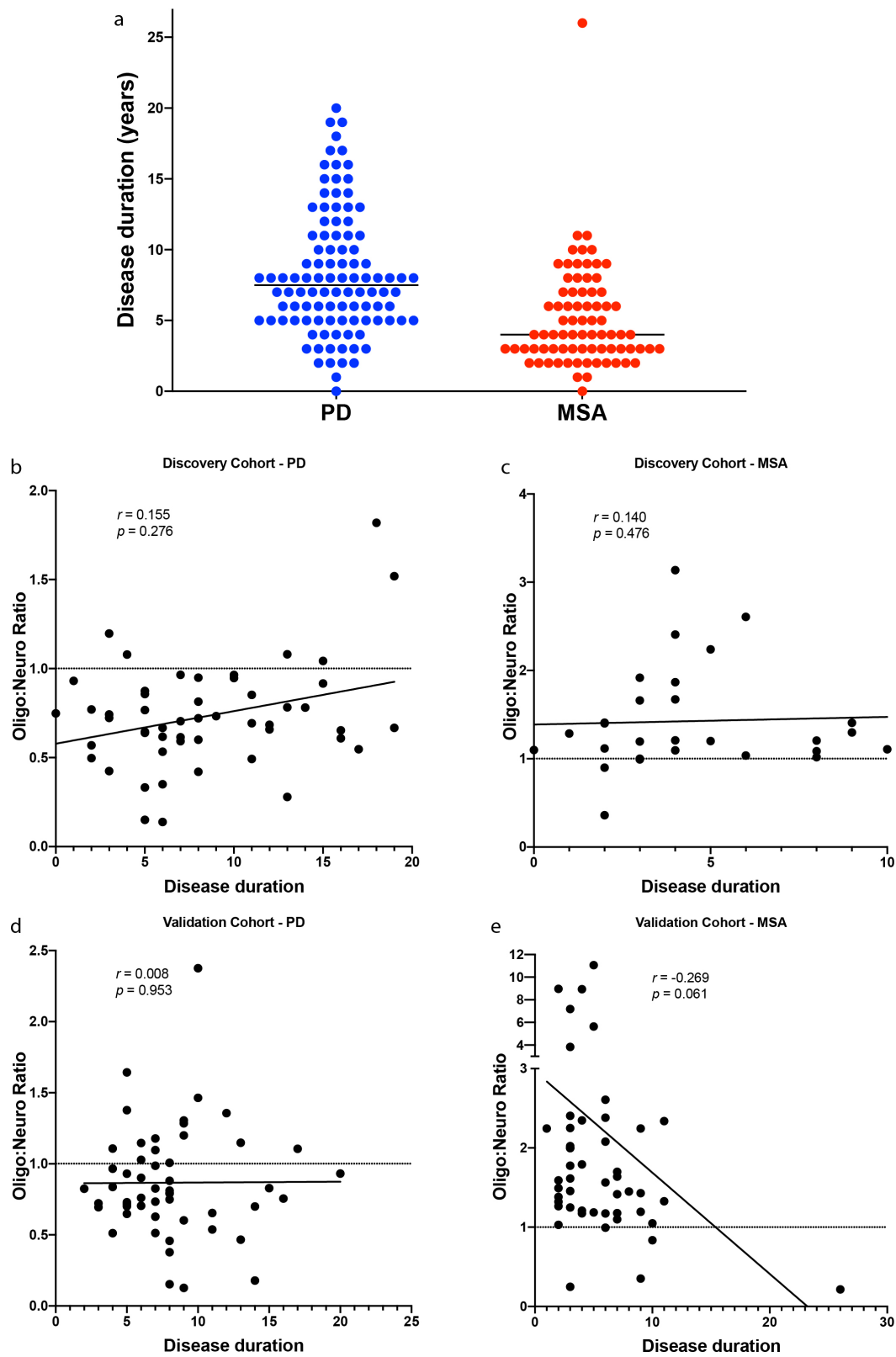
**Supplementary Fig. 10. Measurement of exosome concentration and serum  $\alpha$ -syn before exosome isolation in the validation cohort.** a) Exosome concentration was estimated using a CD81 ELISA. The raw values were converted to exosome concentration according to the



manufacturer’s instructions and log-transformed. b)  $\alpha$ -Syn concentration was measured in 0.5  $\mu$ L serum/plasma using ECLIA and log-transformed. c) Comparison among log-transformed  $\alpha$ -syn concentrations in serum/plasma samples from different sources. P-values were calculated by a one-way ANOVA with post hoc Tukey test.

**Supplementary Table S4. Comparison of statistical models.**

| Model  | Cohort     | Control vs. PD |             |             | Control vs. MSA |             |             | PD vs. MSA |             |             |
|--|------------|----------------|-------------|-------------|-----------------|-------------|-------------|------------|-------------|-------------|
|  |            | AUC            | Sensitivity | Specificity | AUC             | Sensitivity | Specificity | AUC        | Sensitivity | Specificity |
| Multinomial logistic model with LASSO variable selection | Discovery  | 0.762          | 60.8%       | 85.7%       | 0.961           | 96.7%       | 89.8%       | 0.928      | 82.4%       | 93.3%       |
|  | Validation | 0.610          | 71.4%       | 62.7%       | 0.962           | 96.0%       | 84.3%       | 0.902      | 89.8%       | 86.0%       |
| Quadratic discriminant analysis                          | Discovery  | 0.711          | 83.7%       | 57.8%       | 0.956           | 90.8%       | 91.7%       | 0.883      | 90.0%       | 70.6%       |
|  | Validation | 0.597          | 65.7%       | 67.3%       | 0.945           | 83.3%       | 91.0%       | 0.831      | 73.0%       | 82.7%       |
| Classification tree                                      | Discovery  | 0.679          | 72.5%       | 64.7%       | 0.890           | 81.6%       | 90.0%       | 0.891      | 90.0%       | 88.2%       |
|  | Validation | 0.575          | 75.5%       | 43.9%       | 0.890           | 84.3%       | 92.0%       | 0.805      | 92.0%       | 69.4%       |



**Supplementary Fig. 11. The Oligo:Neuro ratio does not correlate with disease duration and can be used for early-stage diagnosis. a) Disease duration distribution for the samples used in**

both cohorts combined. Duration of <1 year was artificially assigned a value of 0. The median values are 7.5 years for PD and 4 years for MSA. b-d) Spearman correlation between the Oligo:Neuro ratio and disease duration in the discovery cohort PD samples (b), discovery cohort MSA samples (c), validation cohort PD samples (d), and validation cohort MSA samples (e).

**Supplementary Table S5. Diagnosis prediction, change, and validation.**

| Sample | Original diagnosis | Change is diagnosis   | Oligo:neuro ratio | Model-predicted diagnosis | Pathologically validated diagnosis |
|--------|--------------------|---|-------------------|---------------------------|------------------------------------|
| 1      | PD                 | PDD   | 1.819             | MSA                       | -                                  |
| 2      | PD                 | MSA-P   | 1.200             | MSA                       |                                    |
| 3      | PD                 | PDD   | 0.931             | PD                        |                                    |
| 4      | Possible MSA-C     | Bulbar-onset ALS  | 2.244             | MSA                       | -                                  |
| 5      | Possible MSA-C     | Probable MSA-C  | 1.997             | MSA                       | -                                  |
| 26     | Possible MSA-C     | Probable MSA-C  | 1.018             | MSA                       | MSA                                |
| 7      | Possible MSA-C     | Probable MSA-C  | 1.209             | MSA                       | -                                  |
| 8      | Possible MSA-C     | Paraneoplastic ataxia due to lymphoma                                       | 1.128             | MSA                       | -                                  |
| 9      | Possible MSA-C     | Possibly acquired cerebellar disorder with superimposed Parkinson's disease | 0.215             | PD                        |                                    |
| 10     | Possible MSA-mixed | -   | 2.381             | MSA                       | MSA + AD                           |
| 11     | Possible MSA-mixed | MSA-C   | 1.456             | MSA                       | -                                  |
| 12     | Possible MSA-P     | Concern for PSP   | 1.918             | MSA                       | -                                  |
| 13     | Possible MSA-P     | Probable MSA-P  | 1.408             | MSA                       | -                                  |
| 14     | Probable MSA-C     | -   | 3.833             | MSA                       | MSA                                |
| 15     | Probable MSA-C     | Possible MSA-C  | 2.245             | MSA                       | -                                  |
| 16     | Probable MSA-C     | -   | 1.492             | MSA                       | MSA                                |
| 17     | Probable MSA-C     | -   | 1.095             | MSA                       | MSA                                |
| 18     | Probable MSA-C     | -   | 1.660             | MSA                       | MSA                                |

|    |                |   |       |     |          |
|----|----------------|---|-------|-----|----------|
| 19 | Probable MSA-C | - | 1.286 | MSA | MSA      |
| 20 | Probable MSA-C | - | 1.037 | MSA | MSA      |
| 21 | Probable MSA-C | - | 0.889 | PD  | MSA      |
| 22 | Probable MSA-C | - | 1.327 | MSA | MSA      |
| 23 | Probable MSA-C | - | 0.351 | PD  | MSA      |
| 24 | Probable MSA-C | - | 5.635 | MSA | MSA      |
| 25 | Probable MSA-P | - | 1.429 | MSA | MSA + AD |

## References

- 1 Angiolini F, Belloni E, Giordano M, Campioni M, Forneris F, Paronetto MP, Lupia M, Brandas C, Pradella D, Di Matteo A et al (2019) A novel L1CAM isoform with angiogenic activity generated by NOVA2-mediated alternative splicing. *Elife* 8: Doi 10.7554/eLife.44305
- 2 Barbour R, Kling K, Anderson JP, Banducci K, Cole T, Diep L, Fox M, Goldstein JM, Soriano F, Seubert P et al (2008) Red blood cells are the major source of  $\alpha$ -synuclein in blood. *Neurodegener Dis* 5: 55-59 Doi 10.1159/000112832
- 3 Beach TG, Adler CH, Sue LI, Serrano G, Shill HA, Walker DG, Lue L, Roher AE, Dugger BN, Maarouf C et al (2015) Arizona Study of Aging and Neurodegenerative Disorders and Brain and Body Donation Program. *Neuropathology* 35: 354-389 Doi 10.1111/neup.12189
- 4 Chettimada S, Lorenz DR, Misra V, Dillon ST, Reeves RK, Manickam C, Morgello S, Kirk GD, Mehta SH, Gabuzda D (2018) Exosome markers associated with immune activation and oxidative stress in HIV patients on antiretroviral therapy. *Sci Rep* 8: 7227 Doi 10.1038/s41598-018-25515-4
- 5 Cholak E, Bugge K, Khondker A, Gauger K, Pedraz-Cuesta E, Pedersen ME, Bucciarelli S, Vestergaard B, Pedersen SF, Rheinstadter MC et al (2020) Avidity within the N-terminal anchor drives  $\alpha$ -synuclein membrane interaction and insertion. *FASEB J* 34: 7462-7482 Doi 10.1096/fj.202000107R
- 6 Coakham HB, Garson JA, Allan PM, Harper EI, Brownell B, Kemshead JT, Lane EB (1985) Immunohistological diagnosis of central nervous system tumours using a monoclonal antibody panel. *J Clin Pathol* 38: 165-173 Doi 10.1136/jcp.38.2.165
- 7 Fiandaca MS, Kapogiannis D, Mapstone M, Boxer A, Eitan E, Schwartz JB, Abner EL, Petersen RC, Federoff HJ, Miller BL et al (2015) Identification of preclinical Alzheimer's disease by a profile of pathogenic proteins in neurally derived blood exosomes: A case-control study. *Alzheimers Dement* 11: 600-607 e601 Doi 10.1016/j.jalz.2014.06.008
- 8 Haspel J, Grumet M (2003) The L1CAM extracellular region: a multi-domain protein with modular and cooperative binding modes. *Front Biosci* 8: s1210-1225 Doi 10.2741/1108

1 9 Helwa I, Cai J, Drewry MD, Zimmerman A, Dinkins MB, Khaled ML, Seremwe M,  
2 Dismuke WM, Bieberich E, Stamer WD et al (2017) A Comparative Study of Serum  
3 Exosome Isolation Using Differential Ultracentrifugation and Three Commercial  
4 Reagents. PLoS One 12: e0170628 Doi 10.1371/journal.pone.0170628  
5 10 Hornung S, Dutta S, Bitan G (2020) CNS-Derived Blood Exosomes as a Promising  
6 Source of Biomarkers: Opportunities and Challenges. Front Mol Neurosci 13: 38 Doi  
7 10.3389/fnmol.2020.00038  
8 11 Kapogiannis D, Mustapic M, Shardell MD, Berkowitz ST, Diehl TC, Spangler RD, Tran  
9 J, Lazaropoulos MP, Chawla S, Gulyani S et al (2019) Association of Extracellular  
10 Vesicle Biomarkers With Alzheimer Disease in the Baltimore Longitudinal Study of  
11 Aging. JAMA Neurol: Doi 10.1001/jamaneurol.2019.2462  
12 12 Mujoo K, Spiro RC, Reisfeld RA (1986) Characterization of a unique glycoprotein  
13 antigen expressed on the surface of human neuroblastoma cells. J Biol Chem 261: 10299-  
14 10305  
15 13 Norman M, Ter-Ovanesyan D, Trieu W, Lazarovitz R, Kowal EJK, Lee JH, Chen-Plotkin  
16 AS, Regev A, Church GM, Walt DR (2020) L1CAM is not Associated with Extracellular  
17 Vesicles in Human Cerebrospinal Fluid or Plasma. BioRxiv:  
18 doi.org/10.1101/2020.1108.1112.247833 Doi doi.org/10.1101/2020.08.12.247833  
19 14 Nuscher B, Kamp F, Mehnert T, Odoy S, Haass C, Kahle PJ, Beyer K (2004)  $\alpha$ -  
20 Synuclein has a high affinity for packing defects in a bilayer membrane: a  
21 thermodynamics study. J Biol Chem 279: 21966-21975 Doi 10.1074/jbc.M401076200  
22 15 Oubrai MM, Wang J, Swann MJ, Galvagnion C, Guilliams T, Dobson CM, Welland ME  
23 (2013)  $\alpha$ -Synuclein senses lipid packing defects and induces lateral expansion of lipids  
24 leading to membrane remodeling. J Biol Chem 288: 20883-20895 Doi  
25 10.1074/jbc.M113.478297  
26 16 Samatov TR, Wicklein D, Tonevitsky AG (2016) L1CAM: Cell adhesion and more. Prog  
27 Histochem Cytochem 51: 25-32 Doi 10.1016/j.proghi.2016.05.001  
28 17 Shi M, Kovac A, Korff A, Cook TJ, Gingham C, Bullock KM, Yang L, Stewart T, Zheng  
29 D, Aro P et al (2016) CNS tau efflux via exosomes is likely increased in Parkinson's  
30 disease but not in Alzheimer's disease. Alzheimers Dement 12: 1125-1131 Doi  
31 10.1016/j.jalz.2016.04.003  
32 18 Shi M, Liu C, Cook TJ, Bullock KM, Zhao Y, Gingham C, Li Y, Aro P, Dator R, He C et  
33 al (2014) Plasma exosomal  $\alpha$ -synuclein is likely CNS-derived and increased in  
34 Parkinson's disease. Acta Neuropathol 128: 639-650 Doi 10.1007/s00401-014-1314-y  
35 19 Tobon-Arroyave SI, Celis-Mejia N, Cordoba-Hidalgo MP, Isaza-Guzman DM (2019)  
36 Decreased salivary concentration of CD9 and CD81 exosome-related tetraspanins may be  
37 associated with the periodontal clinical status. J Clin Periodontol 46: 470-480 Doi  
38 10.1111/jcpe.13099  
39 20 Welker MW, Reichert D, Susser S, Sarrazin C, Martinez Y, Herrmann E, Zeuzem S,  
40 Piiper A, Kronenberger B (2012) Soluble serum CD81 is elevated in patients with  
41 chronic hepatitis C and correlates with alanine aminotransferase serum activity. PLoS  
42 One 7: e30796 Doi 10.1371/journal.pone.0030796  
43 21 Winston CN, Goetzl EJ, Akers JC, Carter BS, Rockenstein EM, Galasko D, Masliah E,  
44 Rissman RA (2016) Prediction of conversion from mild cognitive impairment to  
45 dementia with neuronally derived blood exosome protein profile. Alzheimers Dement  
46 (Amst) 3: 63-72 Doi 10.1016/j.dadm.2016.04.001

1 22 Yan Z, Dutta S, Liu Z, Yu X, Mesgarzadeh N, Ji F, Bitan G, Xie YH (2019) A Label-  
2 Free Platform for Identification of Exosomes from Different Sources. ACS Sens 4: 488-  
3 497 Doi 10.1021/acssensors.8b01564  
4